

**PL-TR-97-2160**

## **REGIONAL SMALL-EVENT IDENTIFICATION USING SEISMIC NETWORKS AND ARRAYS**

**Michael A.H. Hedlin**

**University of California/San Diego  
Scripps Institution of Oceanography  
La Jolla, CA 92093**

**9 December 1997**

**Final Report  
23 June 1995 – 22 September 1997**

**Approved for public release; distribution unlimited**

19980630 028



**AIR FORCE RESEARCH LABORATORY  
Space Vehicles Directorate  
29 Randolph Road  
AIR FORCE MATERIEL COMMAND  
HANSCOM AFB, MA 01731-3010**


SPONSORED BY  
Air Force Technical Applications Center  
Directorate of Nuclear Treaty Monitoring  
Project Authorization T/5101

MONITORED BY  
Air Force Research Laboratory  
CONTRACT No. F19628-95-K-0012

The views and conclusions contained in this document are those of the authors and should not be interpreted as representing the official policies, either express or implied, of the Air Force or U.S. Government.

This technical report has been reviewed and is approved for publication.

  
JAMES C. BATTIS  
Contract Manager

  
CHARLES P. PIKE, Deputy Director  
Integration and Operations Division

This report has been reviewed by the ESD Public Affairs Office (PA) and is releasable to the National Technical Information Service (NTIS).

Qualified requestors may obtain copies from the Defense Technical Information Center. All others should apply to the National Technical Information Service.

If your address has changed, or you wish to be removed from the mailing list, or if the addressee is no longer employed by your organization, please notify AFRL/VSOE, 29 Randolph Road, Hanscom AFB, MA 01731-3010. This will assist us in maintaining a current mailing list.

Do not return copies of the report unless contractual obligations or notices on a specific document requires that it be returned.

REPORT DOCUMENTATION PAGE			Form Approved OMB No. 0704-0188	
Public reporting burden for this collection of information is estimated to average 1 hour per response, including the time for reviewing instructions, searching existing data sources, gathering and maintaining the data needed, and completing and reviewing the collection of information. Send comments regarding this burden estimate or any other aspect of this collection of information, including suggestions for reducing this burden to Washington Headquarters Services, Directorate for Information Operations and Reports, 1215 Jefferson Davis Highway, Suite 1204 Arlington, VA 22202-4302, and to the Office of Management and Budget, Paperwork Reduction Project (0704-0188) Washington, D.C. 20503.				
1. AGENCY USE ONLY (Leave blank)	2. REPORT DATE 9 December 1997	3. REPORT TYPE AND DATES COVERED Final report (6/23/95-9/22/97)		
4. TITLE AND SUBTITLE  Regional small-event identification using seismic networks and arrays		5. FUNDING NUMBERS  PE 35999F PR 5101 TA GM WU AF  Contract F19628-95-K-0012		
6. AUTHOR(S)  Michael A.H. Hedlin				
7. PERFORMING ORGANIZATION NAME(S) AND ADDRESS(ES)  University of California, San Diego Scripps Institution of Oceanography IGPP 0225 La Jolla, CA 92093		8. PERFORMING ORGANIZATION REPORT NUMBER		
9. SPONSORING/MONITORING AGENCY NAME(S) AND ADDRESS(ES)  Air Force Research Laboratory 29 Randolph Road Hanscom Air Force Base, MA 01731-3010 Contract Manager: James Battis/VSB1		10. SPONSORING /MONITORING AGENCY REPORT NUMBER  PL-TR-97-2160		
11. SUPPLEMENTARY NOTES				
12a. DISTRIBUTION/AVAILABILITY STATEMENT  approved for public release; distribution unlimited.		12b. DISTRIBUTION CODE		
13. ABSTRACT (Maximum 200 words)  This report reviews our AFTAC funded research over the last two years. The principal objective of our research was to investigate the utility of time varying spectral estimates obtained from regional seismic records for distinguishing mining events from single explosions and earthquakes. A second goal of this research program was the exploration of additional small-event discrimination techniques which might be merged with the time-frequency method. The emphasis was on acoustic and low-frequency seismic techniques.				
14. SUBJECT TERMS mining explosions, seismic discrimination, time-frequency discriminant, spectral analysis		15. NUMBER OF PAGES 50		
		16. PRICE CODE		
17. SECURITY CLASSIFICATION OF REPORT unclassified	18. SECURITY CLASSIFICATION OF THIS PAGE unclassified	19. SECURITY CLASSIFICATION OF ABSTRACT unclassified	20. LIMITATION OF ABSTRACT  SAR	

## TABLE OF CONTENTS

1. A Global Test of a Time-frequency Small-event Discriminant	2
1.1 The Time-frequency Discriminant – Basic Observations	2
1.2 Display and Automated Recognition of Time Independence Spectra	7.
1.3 Multivariate Discrimination Analysis	8.
1.4 The Data Used in the Global Test	8.
1.5 The ATFD Tested on a Dense 3-Component Network	9.
1.6 The Global Test	11.
1.7 Discussion of Outliers	11.
1.8 A Need for More data	13.
2. Two Ground Truth Experiments in Wyoming-Observations of Anomalous Events	
2.1 The 1996 Wyoming Experiment Overview	14.
2.2 A Ground Truthed Outlier	15.
2.3 A Detonation Anomaly	18.
2.4 Analyses	18.
3. Some Observations of Low Frequency Spectral Modulations	21.
3.1 Time-independent Scallops Below 10 Hz	21.
3.2 Current Work	25.
4. 4. Regional Observations of Time-domain Seismic Source Characteristics	25.
4.1 A Regional “Ms:mb”	25.
4.2 An Obvious Mismatch Between Calibration and Cast Shots	25.
4.3 Current Work	28.
4.4 Waveform Correlation	28.
4.5 Current Work on Waveform Correlation	29.
5. Regional Acoustic Monitoring	30.
5.1 1996 Infrasound Experiment	30.
5.2 A Simulation of the Effect of Wind Shear	30.
5.3 Recommendations	32.
5.4 The 1996 Continuous GPS Experiment: Brief Overview of Results	36.
5.5 Implications for CTBT Monitoring	36.
References	37.
Appendix: The Automated Time-Frequency Discriminant	40.

## Summary

The principal objective of our research over the last 2 years was to investigate the utility of time varying spectral estimates obtained from regional seismic records for distinguishing mining events from single explosions and earthquakes. A second goal of this research program was the exploration of additional small-event discrimination techniques which might be merged with the time-frequency method. The emphasis was on acoustic and low-frequency seismic techniques.

The observation (*Hedlin et al., 1989*) that mine blasts consistently yield spectral modulations that are independent of time, recording component and the azimuth from the source to receiver formed the basis of our work. The original algorithm which looks for these delay-fire diagnostics (described in *Hedlin et al., 1989*) has been tested on a collection of broadly distributed and dissimilar regional datasets. Modifications that took fuller advantage of 3-component network and array data are described in *Hedlin (1997)* and in this report. The modified discriminant is robust, giving misclassification probabilities, estimated with multivariate statistics, ranging from 0.5 to 3.5 percent. Discrimination using time-frequency expansions does not rely on expert interpretation but is routine.

Recent regional experiments in Wyoming, conducted by UCSD, LANL and SMU, have yielded evidence that millisecond delay-fired mining blasts routinely produce significant modulations below 10 Hz. These modulations, which are likely due to source finiteness and not millisecond intershot delays, are similar to those at high frequencies in other events, as they are independent of time, sensor orientation and location. These low-frequency features might be useful for discrimination at mid- to far-regional ranges, but their cause needs to be more thoroughly investigated. The experiments have produced recordings of ground truthed millisecond delay-fired events which did not yield obvious high-frequency scallops. Although attenuation is clearly a factor, ground truth data suggests that the high frequency scallops are further weakened by shot scatter and waveform variability.

The experiment also provided further evidence (in support of observations presented by *Anandakrishnan et al., 1997*) that large cast mine blasts routinely excite significant long period (10 to 20 s) surface waves. The surface waves seem insensitive to the size of the blast; however, the orientation of the shot grid might be important. This report reviews an analysis of four cast explosions and 2 small (12,000 to 16,000 pound) calibration shots. These cast blasts are easily distinguished at regional distances by comparing surface wave and body wave signal amplitudes. A regional variant of Ms:mb is proposed.

A new approach to small-event discrimination was explored in a collaboration with Eric Calais (at CNRS Geosciences Azur), Michelle Hofton and Bernard Minster (Scripps). As part of the Wyoming regional seismo-acoustic experiment we deployed continuous GPS receivers at local to regional distances from the Powder River Basin. The intent was to see if any significant atmospheric signal could be retrieved from within the first acoustic quiet zone. The receivers sense ionospheric perturbations by measuring signal traveltimes from GPS satellites. The receivers detected significant ionospheric perturbations caused by Black Thunder cast blasts. Signals from magnitude 3 cast blasts were comparable in amplitude to those produced by the magnitude 6.7 Northridge earthquake.

We have tested the utility of infrasound for regional monitoring of mining activity. In collaboration with Rodney Whitaker (LANL) a 3 element, 100 m aperture infrasound array was collocated with a seismic station 200 km from the Black Thunder coal mine in Wyoming. This small array recorded coherent signals from a Black Thunder cast blast which yielded a precise bearing estimate - within 2° of the correct azimuth of the mine shot - despite strong cross-winds at the time of the shot. This report describes this result and a preliminary attempt to synthesize propagation of acoustic energy through a windy atmosphere.

## 1. A Global Test of a Time-frequency Small-event Discriminant

### 1.1 The time-frequency Discriminant - Basic Observations

*Hedlin et al. (1989)* made a number of observations about the seismic coda produced by delay-fired events. In recordings made in Kazakhstan there was clear evidence that the mining was not only producing highly scalloped spectra, but these scallops were long lived. They survived the onset phases and persisted long into the coda (Figures 1, 2a). Although this kind of character can be acquired during propagation, for example by resonance in low-velocity strata, it was clear that these features were spawned by the mining technique (Figures 1, 2b). They most likely result directly from the intershot, or interrow, delays or from the spatial and temporal finiteness of the mining shot-sequences.

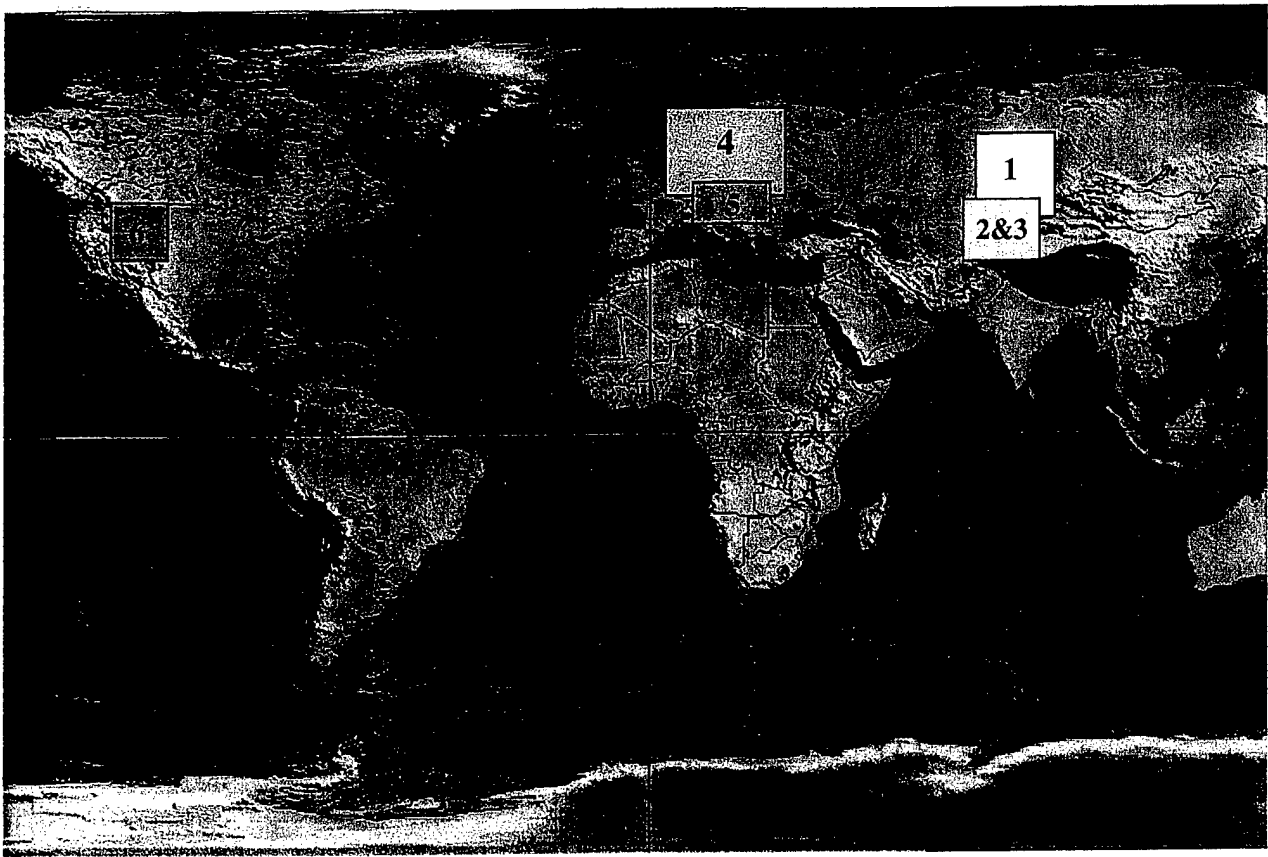


**Figure 1:** All the datasets used in the global test of the discriminant are highlighted. Three kinds of deployments were considered. Networks (1, 2 & 3), tight arrays (4 & 5) and a single, 3-component, station (6). The basemap was obtained from the Cornell group ([http://www.geo.cornell.edu/geology/me\\_na/dataset\\_info/new\\_etopo5.html](http://www.geo.cornell.edu/geology/me_na/dataset_info/new_etopo5.html))

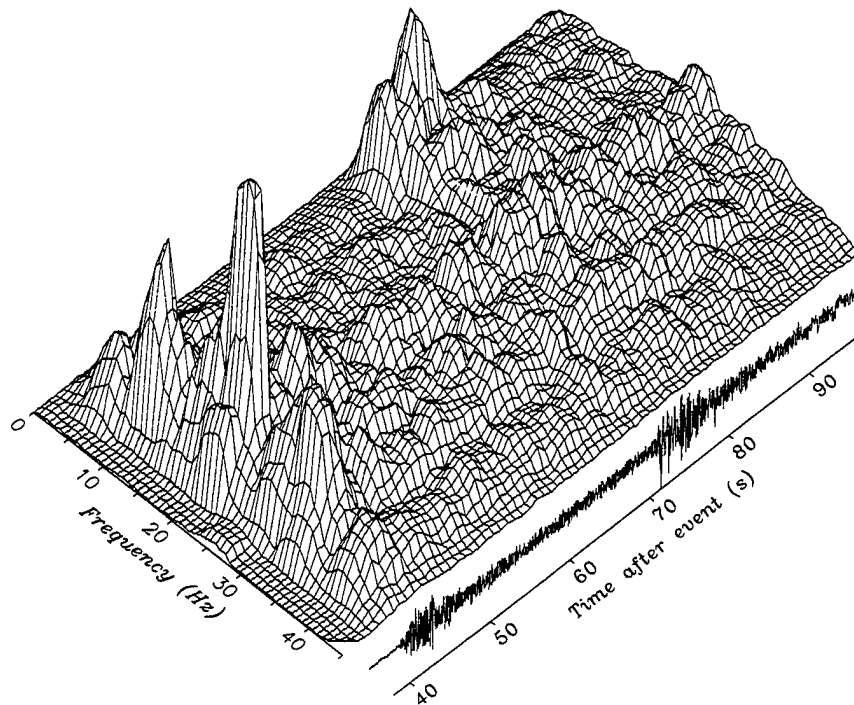


**Figure 2a.** Vertical component seismogram and sonogram from a delay-fired quarry blast (event c; *Hedlin et al., 1989*) detonated in Kazakhstan. The recording was made at a range of 264 km by the vertical component surface seismometer at Bayanaul.

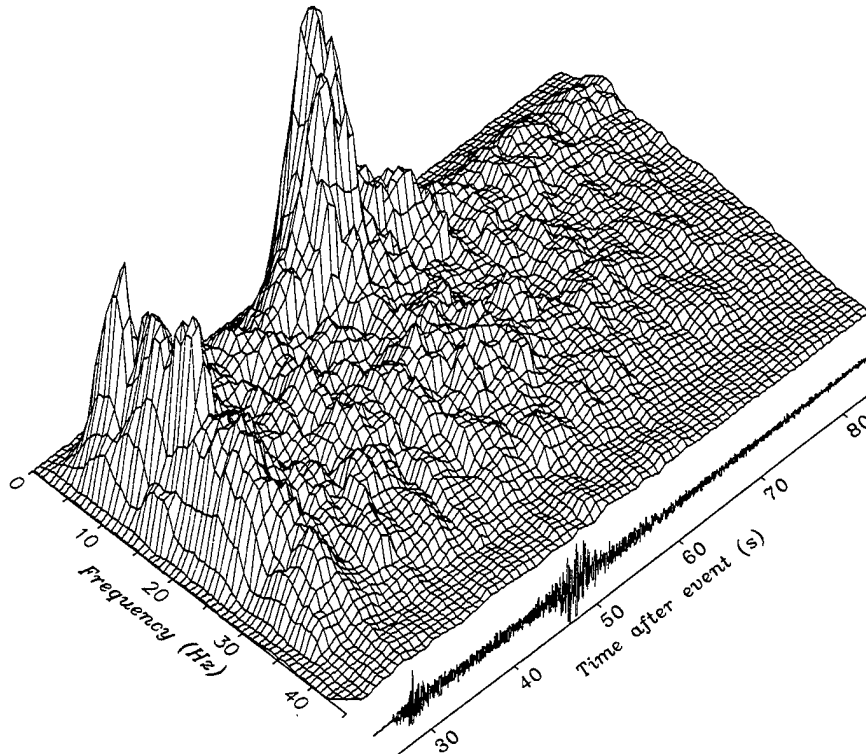


**Figure 2b.** Vertical seismogram and sonogram from a single chemical explosion (chemex 2; *Hedlin et al., 1989*) detonated in Kazakhstan. The recording was made at a range of 157 km by the vertical component seismometer at Bayanaul.

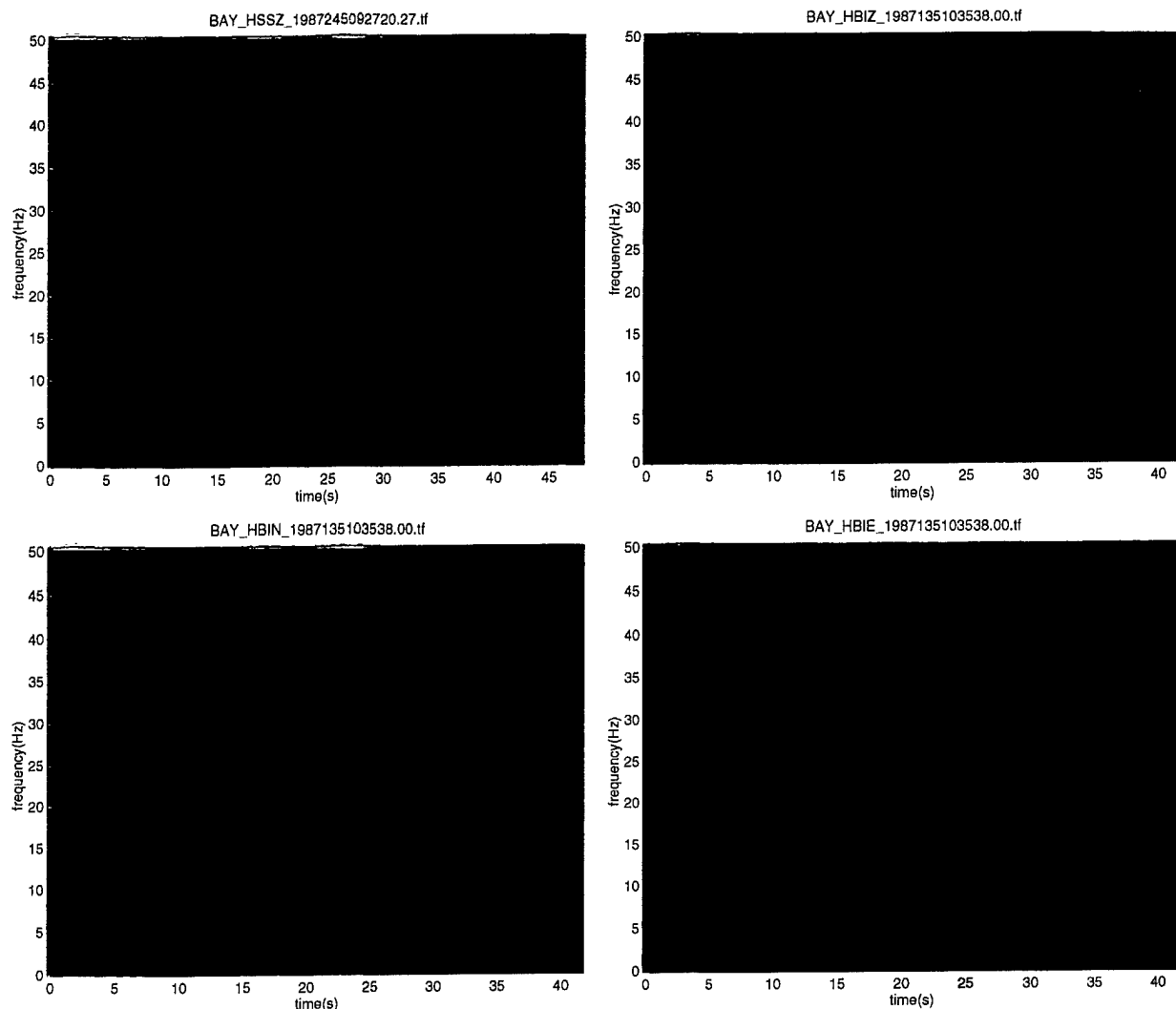


**Figure 3.** *Hedlin et al. (1989)* developed a procedure whereby a binary sonogram is derived from the spectral sonogram by the application of filters which replace spectral information with a binary code which simply reflects local spectral highs and lows. Binary versions of the sonograms presented in Figures 2b and 2a are shown in the upper left and right. Binary sonograms calculated from the north-south and east-west component recordings of the mining explosion (Figure 2a) are shown in the lower left and right.

*Hedlin et al. (1989)* also observed that these scallops were remarkably independent of recording direction and the azimuth from the mine to the receiver. The upper left panel in Figure 3 shows a filtered (binary) version of the sonogram shown in Figure 2b. (see *Hedlin et al., 1989* or the appendix for details on the binary transformation). The other three binary sonograms were obtained from a 3-component recording of the quarry blast shown in Figure 2a. The independence of the scallops from time and recording direction is unmistakable. In Figures 4 and 5, we take this qualitative analysis further and summarize an analysis of recordings of earthquakes and quarry blasts made by the KNET in Kyrgyzstan (*Vernon et al., 1994*). This broadband, 3-component network is ideally suited for our needs since it is situated between the seismically active Tien Shan and a limestone quarry (located just north-east of Bishkek).



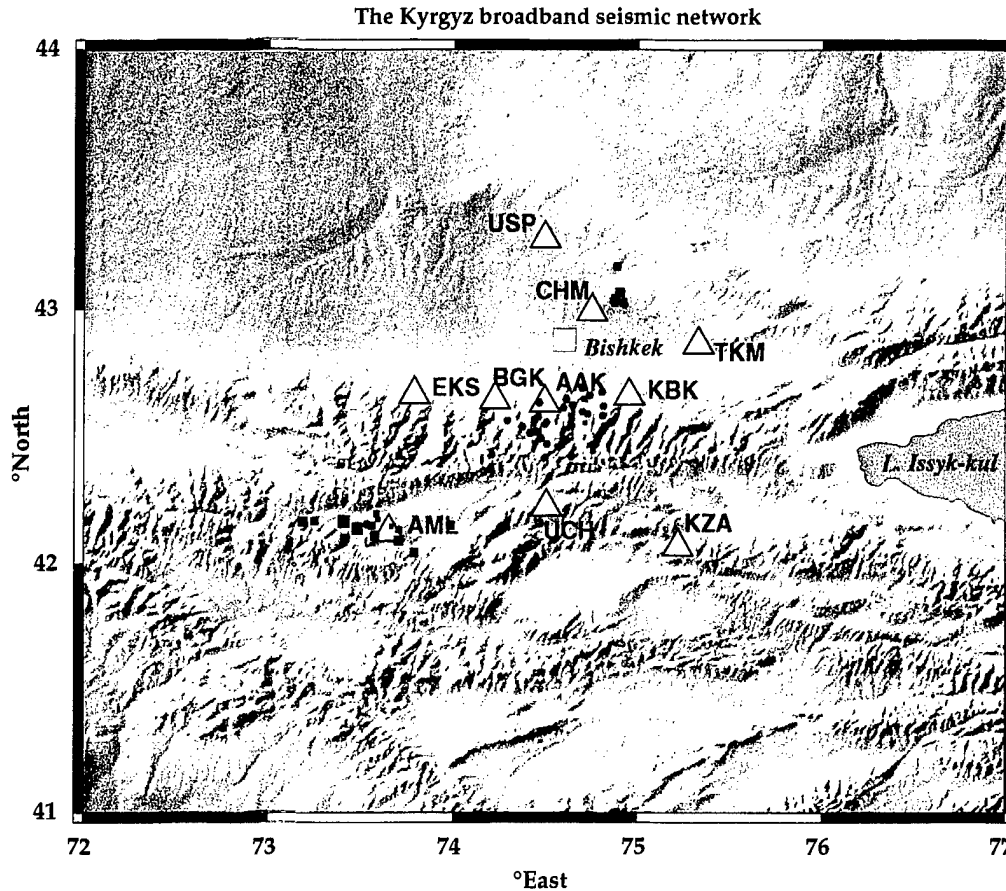


**Figure 4:** The Kyrgyz broadband seismic network. The three clusters of events were used to test the ATFD. The cluster located near station AML are aftershocks to the magnitude 7.3 Sushamyr earthquake. A second cluster of earthquakes is located near AAK. The tight cluster to the northeast of CHM are all believed to be delay-fired shots in a limestone quarry.

Examining the quarry blasts and the cluster of earthquakes located to the southwest of the network (all aftershocks to the  $m_b$  7.3 Sushamyr earthquake; *Mellors et al., 1997*), we found that the network average zero-lag cross correlations of the binary patterns between the recording components (average of east-west vs vertical, vertical vs north-south and east-west vs north-south) clearly separate quarry blasts from earthquakes. A second set of earthquakes (the cluster located within the network) and a second set of quarry blasts from the same mine have essentially the same separation (Figure 5b).

Perhaps these basic observations of independence of scalloping from recording direction and source-receiver azimuth are not surprising. Assuming that the wavefields produced by each sub-shot are identical, evidence of the shot pattern (separation in time and space of many sub-shots in a delay-fired source) should be contained within the recorded, summed wavefield unless the sensor is located so far from the source that frequencies required to document the delays are attenuated. This repetition of a common, single shot wavefield should not depend on the orientation of the sensor since regardless of what happens during propagation between the source and receiver, the information produced by any of the single shots is encoded within the cumulative waveform in the same way. Given that the spatial

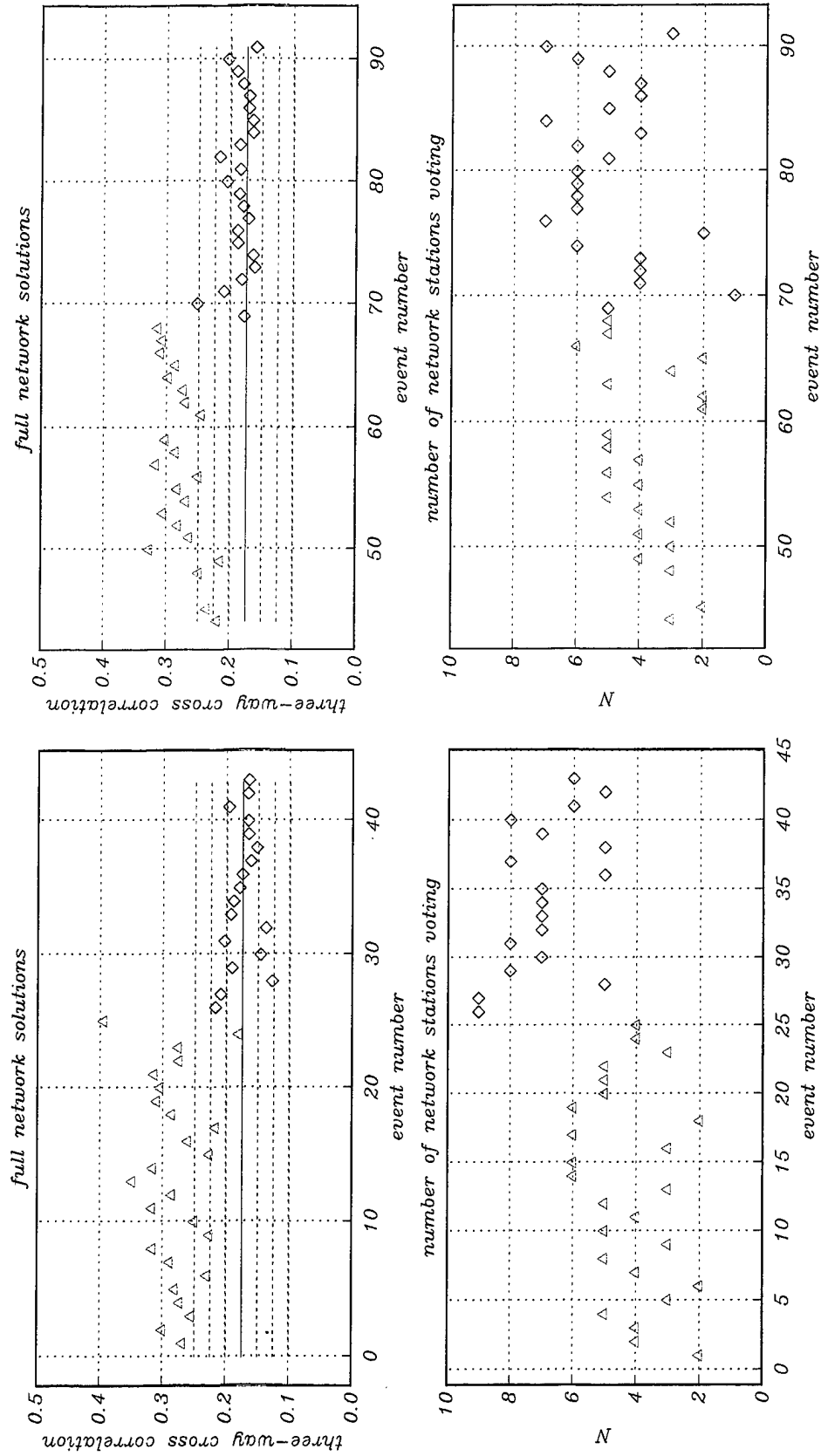


**Figure 5a and b.** Network averaged three-way crosscorrelations calculated using the events in dataset 2 (left figures) and 3 (right). We find that the network solutions exhibit little crossover between the two event types. Using the earthquakes in dataset 2, we have calculated a mean and  $\pm 1, 2$  and 3 standard deviations. These statistics are overlain on the network solutions from dataset 3, showing that the cross-correlations of the two sets of events are essentially the same.

dimensions of the shot-grid are insubstantial, so that the apparent, additional time-delays incurred by the seismic energy propagating between sub-shots are small when compared with the source-time differences, this information should not have a strong dependence on azimuth. Given the conditions just stated, it should be possible to reach the same inferences about the timing of the shot-grid regardless of the orientation of the sensor and its azimuth from the source.

## 1.2 Display and Automated Recognition of Time-independent Spectra

The Automated Time-Frequency Discriminant (ATFD) has been partially described in earlier papers (*e.g. Hedlin et al., 1989; Hedlin et al., 1990; Hedlin et al., 1995*), and only a brief review will be given here. The technique depends on time-frequency displays calculated using Short Time Fourier Transforms (STFT; *Daubechies, 1996*), otherwise known either as sonograms or spectrograms (Figures 2 and 3). An obvious advantage of a single Fourier transform of an entire time-series is that it yields a high resolution spectrum (since the Rayleigh spacing is equal to the inverse of the time-span of the series transformed). The spectral structure of long-lived features is well, if not precisely, defined. The disadvantage is that the spectrum shows an integration of contributions made by many different features in the seismogram - many of which were short lived. The single spectrum doesn't reveal the relative timing of the features and will not allow us to discriminate between short- and long-lived features. Although the STFT provides poorer frequency resolution, it separates early and late transients and thus reveals the evolution of the signal's spectrum with time. It has been pointed out by many authors that the STFT offers time-frequency resolution that is invariant with frequency and that this is at odds with the physics of the signal since, one would expect, high-frequency transients can be short-lived relative to their low-frequency neighbors. Expansion techniques that use wavelets which traverse the time series by translating in time and scaling in frequency offer flexible time- and frequency-resolution (*Daubechies, 1990; 1996*). As frequency ( $f$ ) increases, the length of the wavelets decreases, allowing a closer look at variations with time, and the resolution in frequency becomes poorer ( $\Delta f \Delta t$  conserved). Although the fine details of the time-frequency structure are interesting, and will be used to study the genesis of spectral overtones in a forthcoming paper, what we want for the automated discriminant is a routine process which will tell us if certain frequency bands are enriched in energy while others are depleted. We are seeking spectral modulations which can be long-lived (many periods) regardless of their frequency and are not attempting to precisely define the structure. Also, these modulations result from the multiplication with a modulation function which does not usually scale in bandwidth systematically with frequency. For these reasons, and the fact that wavelet expansions are time consuming and that we are seeking an algorithm which can calculate the expansions of frequent events on the fly, we have continued to use STFT's.

The current ATFD recognizes long-lived modulations in the binary sonograms (*Hedlin et al., 1989*) by applying three separate and simple tests. *Hedlin et al. (1990)* developed a procedure to automatically recognize time-independent patterns which are periodic in frequency. This technique utilizes a two-

dimensional Fourier transform of the binary sonogram which reveals the dependence of the binary pattern on frequency and time. In view of its resemblance to the cepstrum (which identifies periodicities in single spectra), and the fact that it is derived from onset and coda phases we now refer to it as the coda cepstrum (*Hedlin et al., 1995*). The algorithm estimates the time-independence of the binary patterns by calculating the autocorrelation of individual narrow band (single frequency) timeseries. Independence from recording direction is judged by cross-correlation. These operations (reviewed in detail in the appendix) are easily adapted to different kinds of deployments, *e.g.* single component/station to 3C to single or 3C networks or arrays. The algorithm will compute whatever is possible given the deployment - *e.g.* a single vertical component station will yield single estimates of the autocorrelation and the coda cepstrum, a 3-component network will yield a total of 9 network averaged variates.

### 1.3 Multivariate Discrimination Analysis.

These individual parameters are merged into a single discrimination score with the aid of multivariate statistics (*Seber, 1984*). Generally, a linear discriminant function was used unless the dispersion matrices of the two event types were judged to be too dissimilar - in which case a quadratic is appropriate. In all cases, it was assumed that the probability of each event type was equal and the discriminant decision was simply based on the sign of the discriminant function (as in *Kim et al., 1993*). In all cases, standard tests were applied to ensure the validity of the statistical analysis.

### 1.4 The Data Used in the Global Test

Often a discriminant is tested with great success against a single dataset only to perform poorly on a dataset collected elsewhere. There are a number of explanations for this (*e.g.* some discriminants will work well only in certain geological settings). For this reason, this report describes a test of the adaptability of the discriminant using a number of well separated and dissimilar datasets. The algorithm is tested using dissimilar styles of seismic deployment (*incl.* a single 3-component station, single- and 3-component networks and arrays), varying seismic instrumentation (*incl.* short period and broadband) located in distinct tectonic regions where mining techniques are likely to be tailored to local needs. The six datasets are described below and in Figure 1. A full review of the analysis of one dataset follows along with a summary of the rest.

- 1) Single (chemical) explosions and quarry blasts recorded at close range (< 300 km) by a sparse 3-component network (NRDC) deployed in 1987 on a high Q crust in central Kazakhstan (*Berger et al., 1987*). In the absence of in-mine (ground truth) information event identification was based on C. Thurber's interpretation of SPOT photos (*Thurber et al., 1989*) and the fact that the Kazakh platform is seismically quiet (*Berger et al., 1987*).

2&3) Earthquakes and quarry blasts recorded by a dense (10 stations in an aperture of 200 km) telemetered 3-component broadband network (KNET) deployed in Kyrgyzstan on the thrust belt between the Kazakh platform to the north and the seismically active Tien Shan to the south (Figure 4). The analysis uses 100 sps recordings of two clusters of earthquakes and two sets of quarry blasts which occurred at a limestone quarry (located by Rob Mellors, UCSD, at 43.028° N and 74.888° E). Events were identified as quarry blasts on the basis of their location and the origin time - the limestone shots typically occurred in the late afternoon. In addition, some of these events produced obvious acoustic signals which arrived at CHM roughly 37 s after *P*; no ground truth data were available.

4) Recordings of quarry blasts and earthquakes made by the NORESS small aperture array in southern Norway. NORESS consists of 25 GS-13 stations (all vertical except 4 which have 3-components) deployed in a 3 km aperture on Precambrian or Paleozoic hard-rock (*Mykkeltveit et al., 1983*). This dataset consists of 40 sps recordings of 26 quarry blasts (with no ground truth) and 16 earthquakes located within 7.5° of the array (*Hedlin et al., 1990*).

5) Recordings of quarry blasts and earthquakes made by GERESS (*Harjes, 1990*). These recordings were obtained from the European Ground Truth Database (*Grant & Carabajal, 1995*) and were contributed by J. Wuster. Included are 40 sps recordings of 11 quarry blasts and 10 earthquakes located between 1.5 and 2.5° to the northwest of the array (see *Wuster, 1993* for a fuller description).

6) Recordings of quarry blasts (in the Newmont Gold Mine in Nevada) and earthquakes (including events in the Rock Valley earthquake sequence near NTS) made by a single (3-component) broadband Guralp (ELK in the LNN network) located near Carlin, NV roughly 80 km from the mine (*Jarpe et al., 1996*). The sensor has a flat response to velocity between 0.01 and 30 Hz. The hard rock mine (which detonates delay-fired shots every 2 days each using 15 to 100 tons of explosives) has been monitored by LLNL scientists (*incl. Drs. Peter Goldstein, Bill Moran and Steve Jarpe*). Mining records have been used to constrain the blast patterns, which typically involve delays from 50 to 100 ms. This dataset, contributed to us by Steve Jarpe and Peter Goldstein, consists of 42 quarry blasts (all occurring at the Newmont Gold Mine in Nevada) and 36 widely dispersed earthquakes all located within 2° of ELK (*Jarpe et al., 1996*).

### 1.5 The ATFD Tested on a Dense 3-component Network

To illustrate the technique we discuss the analysis of the third dataset (collected by KNET; Figures 1 and 4). The upper two and lower left panels of Figure 6 display the raw output from the ATFD. These panels show that the earthquakes and quarry blasts are separated reasonably well by each of the metrics applied by the ATFD. The lower right panel shows the discriminant scores obtained from three separate linear multivariate analyses. The scores represented by the plus signs are "fitted" (each event was

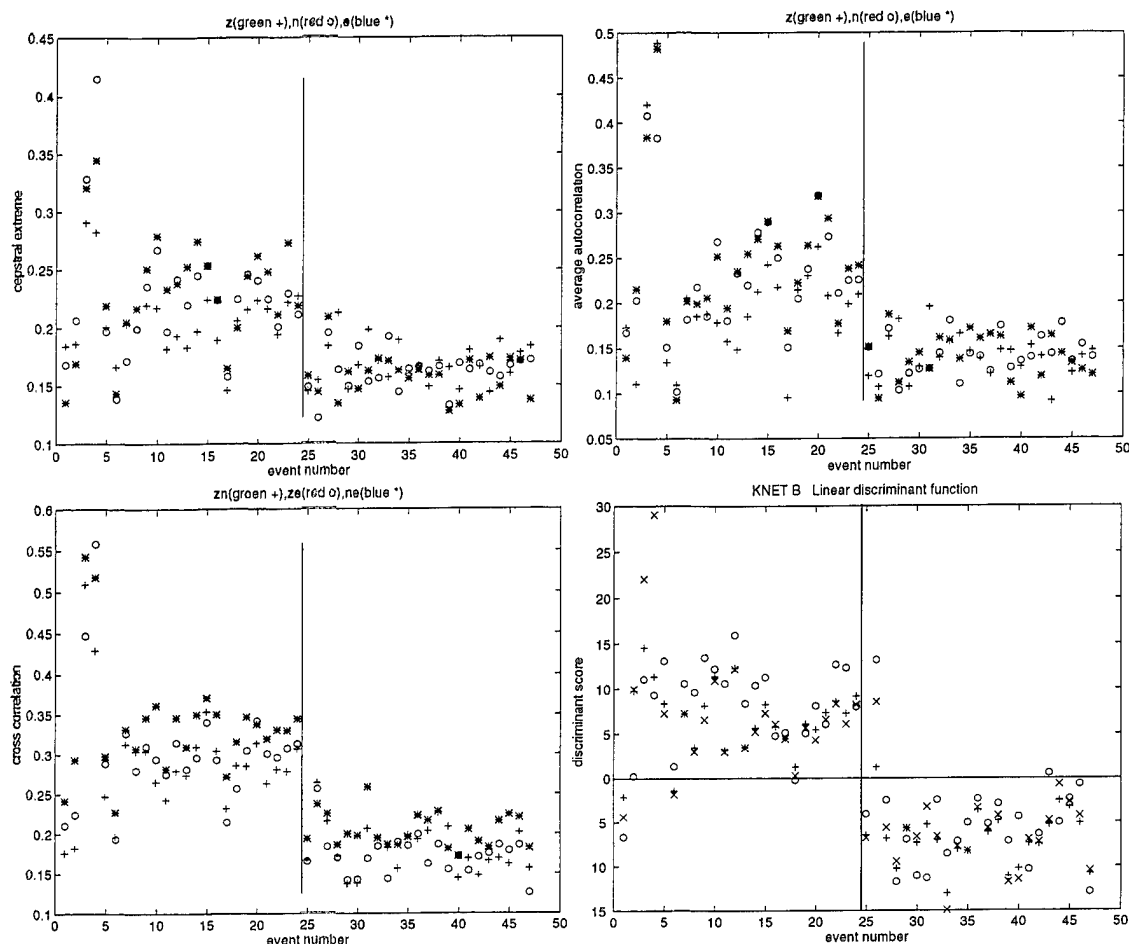


**Figure 6:** The top two and lower left figures show raw variates output by the ATFD in an analysis of the third dataset. Events 1 through 24 are quarry blasts, 25 through 47 are earthquakes. All are plotted relative to a perfect score of 1. For example, a time-frequency matrix that is perfectly periodic in frequency and independent of time (at all stations in the network) would have a cepstral extreme of 1.0. Each event has 9 raw parameters - three plotted in each of the three sub-figures. For example, in the upper left are the network averaged cepstral extremes obtained from the vertical, north-south and east-west components. While there is a wide scatter between the three plotted symbols a clear separation exists between the two event types. The linear discriminant scores are displayed in the lower right. Fitted and drop 1 scores are represented by plus signs and crosses respectively. Scores obtained with the discriminant function from the second dataset are represented by the circles. The two populations are clearly separated.

judged by the discriminant function it was used to define). Of the 47 events, one earthquake and two quarry blasts were misclassified. Following *Lachenbruch & Mickey (1968)* "drop 1" scores (where an event was judged by a discriminant function defined by all events except itself) were also calculated. These scores, represented by the crosses, are slightly worse. The third test used the linear discriminant function derived from the second dataset (same quarry but a different swarm of earthquakes). Surprisingly, the separation between the populations, represented by the circles, is just marginally worse. The second and third tests suggest that the algorithm should be relatively easy to train. The misidentified events were recorded by relatively few stations (events 45, 50 & 70 in Figure 5b) suggesting a low signal-to-noise and little, if any, network averaging. Outliers, such as these, are a critical problem and are discussed in more detail in the next section.

## 1.6 The Global Test

The raw output of the ATFD for all 250 events considered in this study are shown in Figure 7. The results are organized into 3 panels giving the autocorrelation, cross-correlation and coda-cepstrum extremes. Again, in each panel the quarry blasts are displayed with the left (events 1 through 144) with the single explosions and earthquakes on the right (events 145 to 250). The datasets are color coded from left to right (*e.g.* compare the red symbols to assess the performance of the technique on NRDC data). Since all datasets had at least one 3-component sensor, each event is described by 9 variates. Although some overlap exists, the delay-fired events are separated from the earthquakes and single explosions by each of the metrics. The ATFD, when presented with network data, responds in a consistent fashion - the first three datasets cluster in the same manner. The same is true for the tight array data (datasets 4 and 5), which seem to offer less averaging and greater scatter of the variates than the networks. The greatest scatter exists in the single 3-component station results (dataset 6). The discrimination scores are presented in Figure 8. Of the 232 events in datasets 2 through 6, all but 6 were correctly identified. Of the 18 events in the NRDC dataset, it appears that 2 (of the quarry blasts) would likely have been misclassified. The misclassification probabilities ranged from 0.5% (GERESS) to 3.5% (KNET). The ATFD is robust and easily adapted to a wide range of deployments (from single stations to arrays and networks) and thus easily automated.

## 1.7 Discussion of Outliers

Although the misclassification statistics quoted above are promising, the time-frequency discriminant, like any other, is not perfect - it alone is not the antidote for the small event discrimination problem. Some of the events may have been misclassified because they were misidentified in the first place - *i.e.* the algorithm is simply correcting the *apriori* information. Perhaps a few mining events were misidentified because millisecond delays were not used. It seems more likely that the *apriori* identifications are correct; that is, millisecond delays were used and errors have been made because of some inadequacy of the approach. There is much to be learned from the mistakes - what is the physics underlying the outliers? Why are some earthquakes judged to be delay-fired explosions? Why would millisecond delay-fired events sometimes not yield high frequency modulations?

There are a number of ways to explain the absence of scallops. As pointed out by *Stump et al. (1994; 96)*, even though an intended shot-grid might be regular in time, shot-scatter may be substantial enough to eliminate the constructive interference necessary to produce scallops. For reasons as yet unknown, some mine blasts detonate, in part, sympathetically (simultaneously). Energy released instantaneously couples very efficiently to seismic and would likely obscure modulations produced nearby by a delay-fired shot sequence. If significant variability between the basic wavefields exists (*e.g.* as discussed by *Baumgardt, 1996*), the time-stagger will still be in the recorded wavefield but perhaps difficult to extract since the wavefield will contain stagger without repetition. A fourth and obvious cause of the absence of scallops is attenuation which will preferentially strip the higher frequencies out of the

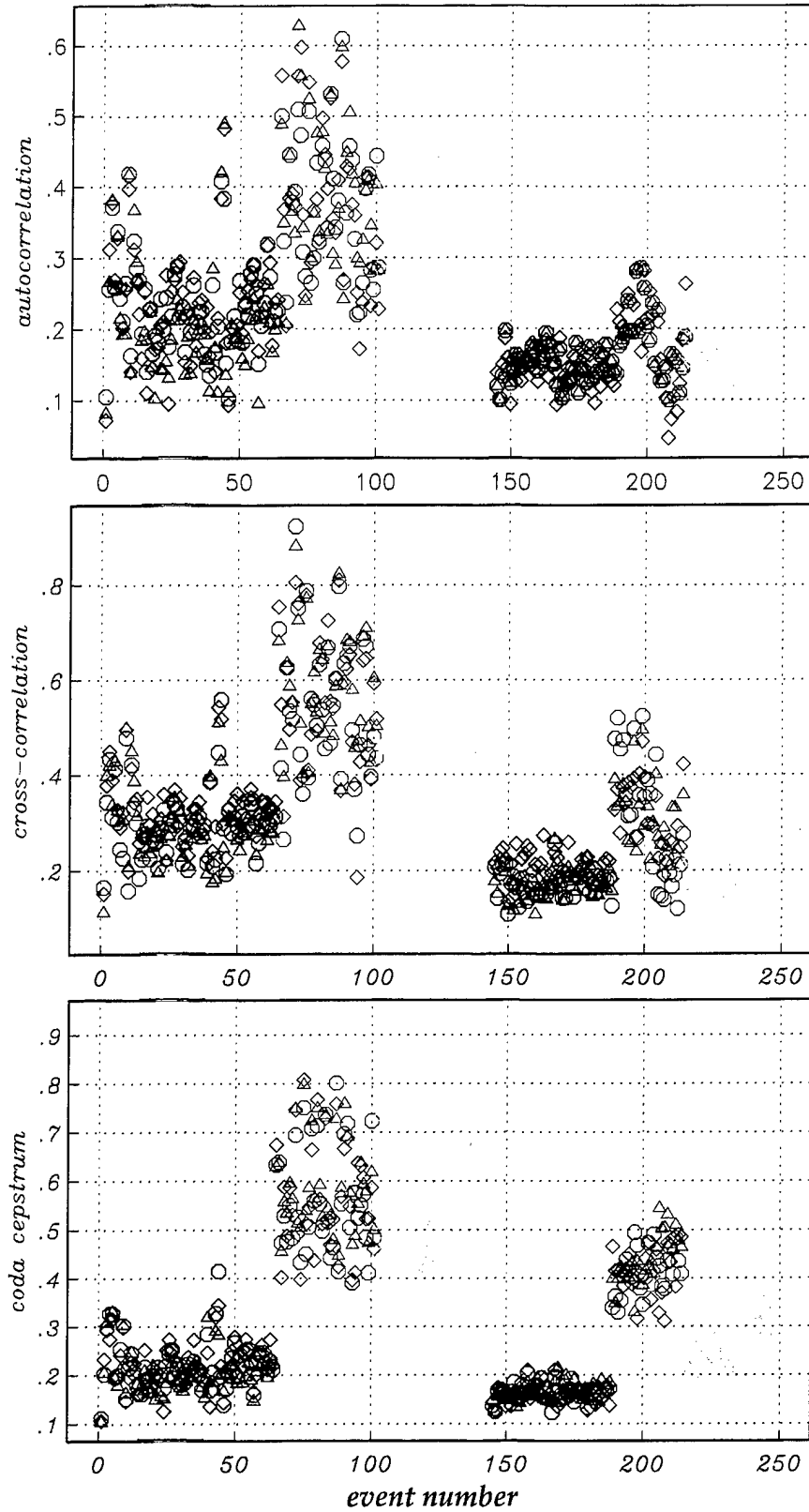


**Figure 7:** Raw output from the ATFD for all 250 events considered in this study. Events believed to be quarry blasts are located on the left (1 through 144) and the single explosions (NRDC only) and earthquakes are located on the right. The three discrimination methods (autocorrelation, cross-correlation and coda-cepstra extremes) are shown from top to bottom. The datasets are arranged from left to right in order (Figure 1).



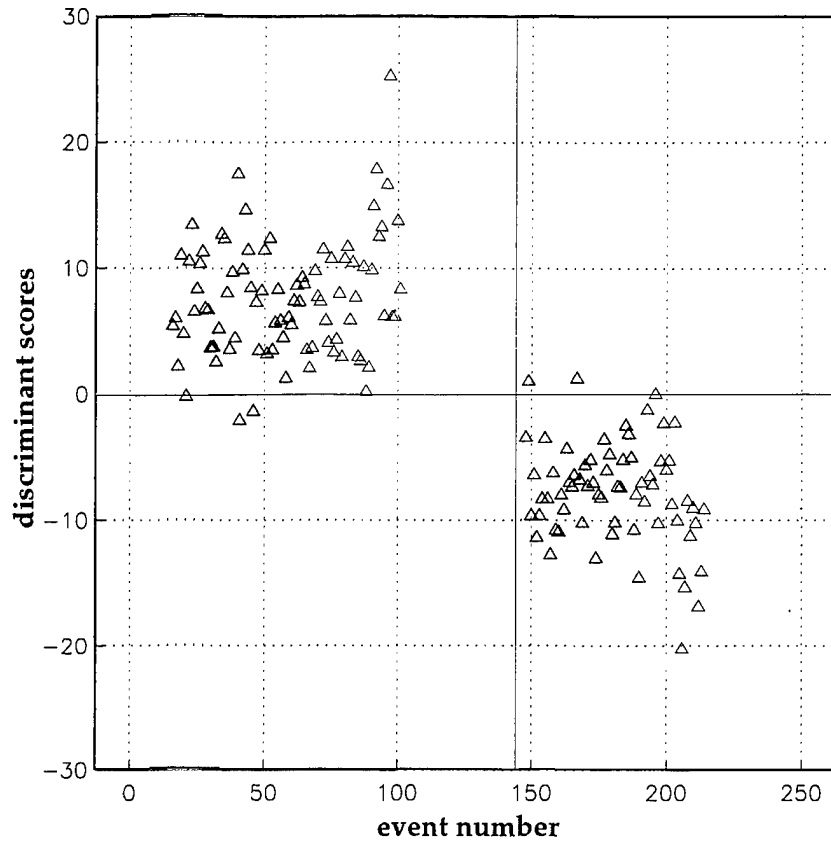


**Figure 8:** Discriminant scores from datasets 2 through 6. The NRDC scores haven't been included since there were too few explosions (3) to permit a statistical evaluation. Linear discriminant functions were used for all datasets except the sixth (collected by the single station). The raw parameters suggest that 2 of the 15 quarry blasts in the NRDC dataset would be misidentified. Of the 232 events in the other datasets, all but 6 were correctly identified. As expected, the scatter increases as averaging becomes less effective (single 3-component station).

wavefield. Figures 5 and 6 suggest that the outliers in the KNET datasets exist because too few stations were available for the analysis. This in itself suggests that the events generated little signal (and thus scallops) above noise and that network averaging could not be used. This is clearly not a full explanation, however. There is considerable scatter of the variates calculated from the quarry blasts recorded by 6 stations (Figures 5 and 6). These blasts all occurred in the same limestone quarry. Although waveform decorrelation cannot be ruled out as a cause of this variability, it is easier to invoke simple time scatter, which is known to be common. The flip side of the outlier problem is the appearance of time-independent spectral modulations in earthquake coda. Such modulations might be acquired during resonance in low velocity layers in the crust (*Sereno & Orcutt, 1985*).

### 1.8 A Need for More Data

The issue of outliers is of fundamental importance to the development of this, or any other, discriminant. In this case the problems cannot be adequately addressed since most datasets offer little, if any, ground truth information (the exception is the LLNL dataset which seemed to lend itself particularly well to this discriminant). To advance, we must be able to explain why the discriminant might fail in the

operational setting. To do so we need to analyze well constrained events which are known not to produce high-frequency modulations.

### **Acknowledgments**

The global test and software development wouldn't have been possible without funding provided by AFTAC under contract F19628-95-K-0012. The data used in this section were provided by numerous people. Lori Grant provided us with the European Ground Truth Database which included data donated by J. Wuster. The NORESS data was made available by Tom Sereno at SAIC. The KNET and NRDC datasets were provided by Frank Vernon. Peter Goldstein and Steve Jarpe at LLNL provided the Nevada data. Rob Mellors provided information on the limestone quarry in Kyrgyzstan.

## **2. Two Ground Truth Experiments in Wyoming - Observations of Anomalous Events**

Little of the data used in the global test was collected with ground truth information. In order that progress could be made in a number of the key areas (*incl.* explaining outliers, finding other discriminants) UCSD and LANL jointly conducted two regional seismo-acoustic monitoring experiments in 1996 and 1997 in Wyoming. One advantage in using data from this region is that it contains numerous active mines. Each mine employs a variety of blasting techniques which span many of the practices used globally. Also, these data sets were collected to explore the interplay of several monitoring technologies (video, acoustic & seismic) at local to regional distances from the source. In part, we have collected these data to explore the characteristics of these mining explosions that may provide the robust identification. The experiments illustrate some problematic issues which exist in spite of the close scrutiny of a single region. The overall experiment is reviewed in this section. The acoustic component is discussed in detail in Section 5.

### **2.1 The 1996 Wyoming Experiment Overview**

In the 1996 experiment, five broadband (STS2) seismic stations were placed around the Black Thunder coal mine in eastern Wyoming (Figures 9a and 9b). Four of the stations were at a range of 200 km, the fifth (KRET) was located at a range of 100 km on the same azimuth as one of the outer ring stations. A three-element infrasound array (Section 5) was co-located with the seismic instrument at MNTA. Continuous GPS receivers were located with 200 km from Black Thunder (Section 5). The 1997 regional network mirrored the previous one except no temporary acoustic equipment was used and just four seismic stations (in the outer, 200 km, ring) were deployed. The temporary deployments were in addition to permanent stations (including PDAR). Although the Powder River basin mines are extremely active, the events of greatest interest to us were the extensive cast and calibration shots located in the south pit of the Black Thunder coal mine (*Pearson et al., 1995; Stump, 1995*), as these were closely monitored with video and acoustic equipment by the LANL team. Four cast explosions were recorded

### WY96 Regional Deployment

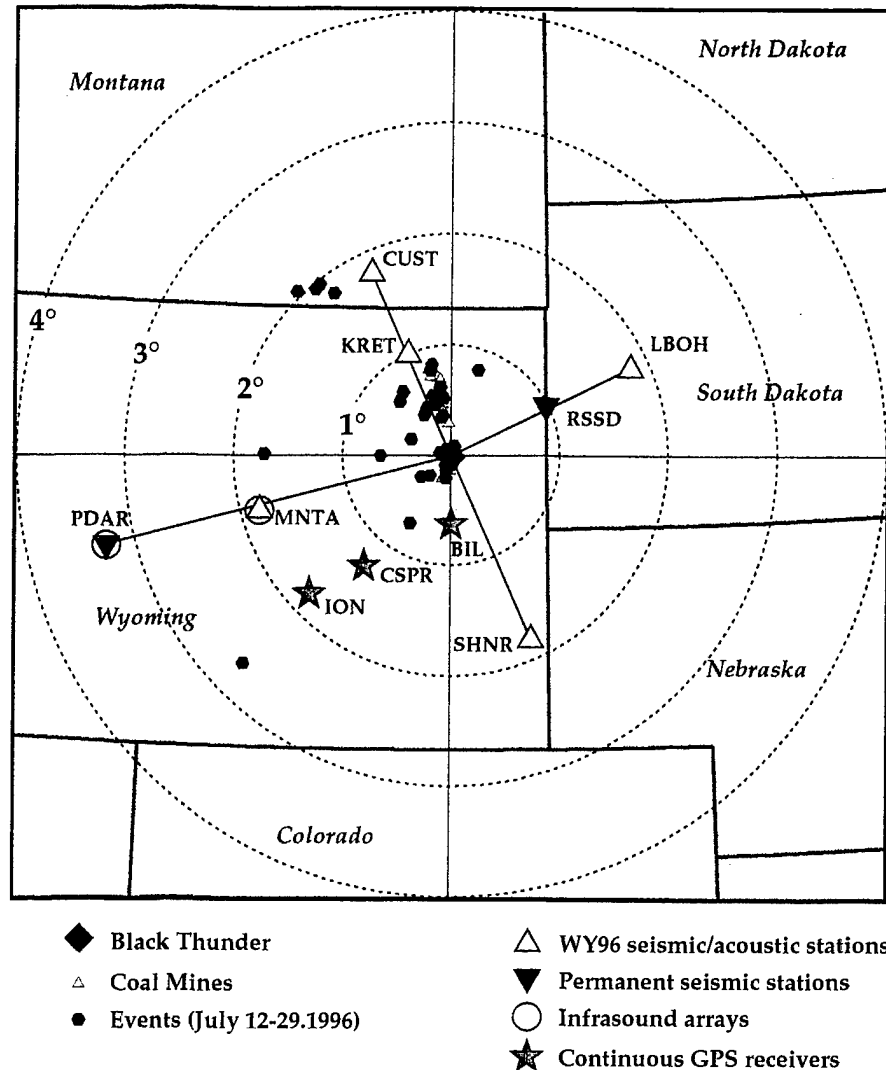


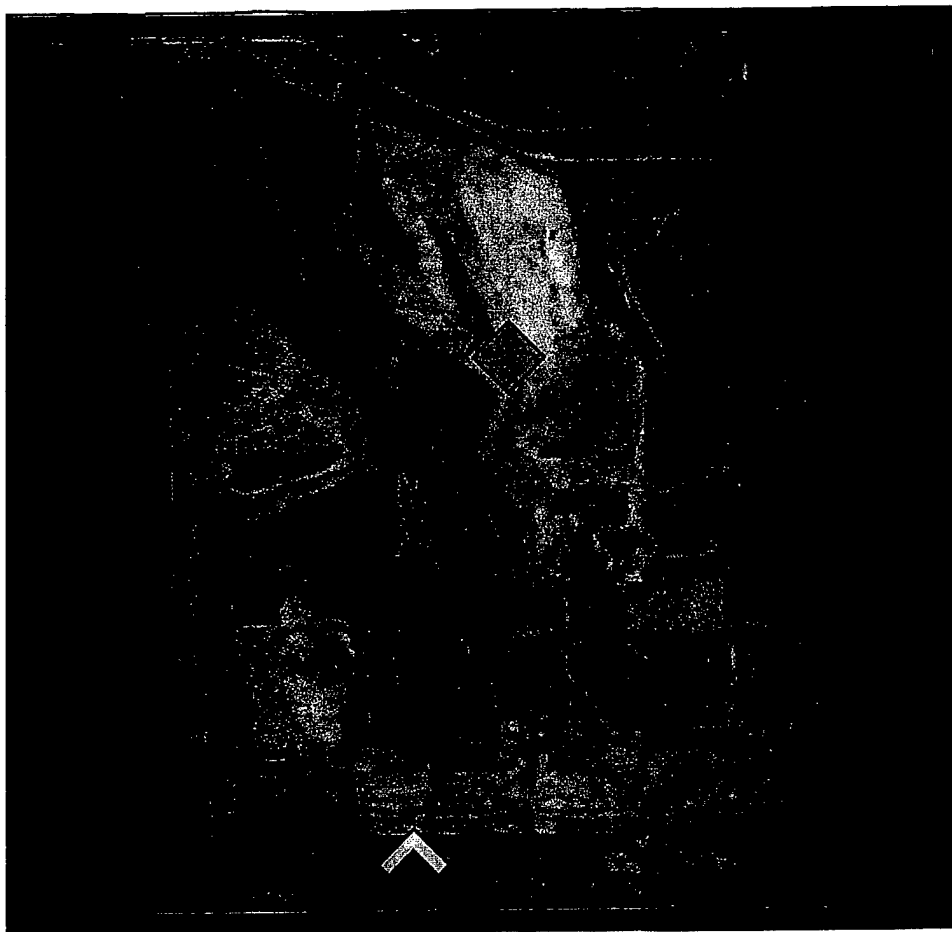
**Figure 9a:** The 1996 Wyoming regional deployment. Although this paper is concerned with seismic results, the deployment also consisted of a three station (100 m aperture) infrasound array located at MNTA and continuous GPS receivers placed at 3 sites. The GPS receivers were deployed to scan for ionospheric perturbations caused by the the acoustic pulse rising from mine shots (Calais *et al.*, 1997). Two of the receivers were located within the first quiet zone where infrasound would likely be ineffective.

during the two experiments. The largest (August 14, 1997; Figure 9b) used ~7 million pounds of ANFO. The calibration shots ranged in size from 5500 pounds to 16,000 pounds (Figure 9b).

### 2.2 A Ground Truthed Outlier

The multi-million pound shots are used to fragment and cast overburden to expose the coal seam. A typical cast shot will consist of ~300 shots arranged in 7 rows detonated within 4 s. Intershot delays of 35 ms and interrow delays of 235 ms (unpublished Black Thunder mine blasting report for cast shot on Aug 1, 1996) suggest modulations at every 4.2 and 30 Hz. Waveforms recorded by stations in the 200 km ring seem to be highly dependent on source-receiver azimuth with, as expected (due to previous observations by Stump and colleagues at LANL), faint, or no, broadband spectral modulations (Figure

## *The Black Thunder Mine*



- |                   |                            |
|-------------------|----------------------------|
| ◇ July 19.1996    | ◆ August 2.1996            |
| ◆ August 1.1996   | ◆ August 14.1997           |
| ★ Observation pt. | ■ 12,000 & 16,000 lb shots |

**Figure 9b.** A satellite photo of the Black Thunder Coal mine in Wyoming. The symbols give approximate locations of the major events considered in this and the following analyses. The 1996 and 1997 experiments produced recordings of 4 significant cast blasts in the Black Thunder coal mine. The July 19, Aug 1, 96, and Aug 14, 97 blasts occurred at the west end of the south pit. The tail end of the Aug 1 blast (shown in red) is believed to have detonated simultaneously. In the July 19, Aug 1, Aug 2 (all 1996) and Aug 14 (1997) cast blasts 4.5, 2.5, 2.8 and 7.0 million pounds of ANFO were detonated. The two largest calibration shots used 12,000 and 16,000 pounds.

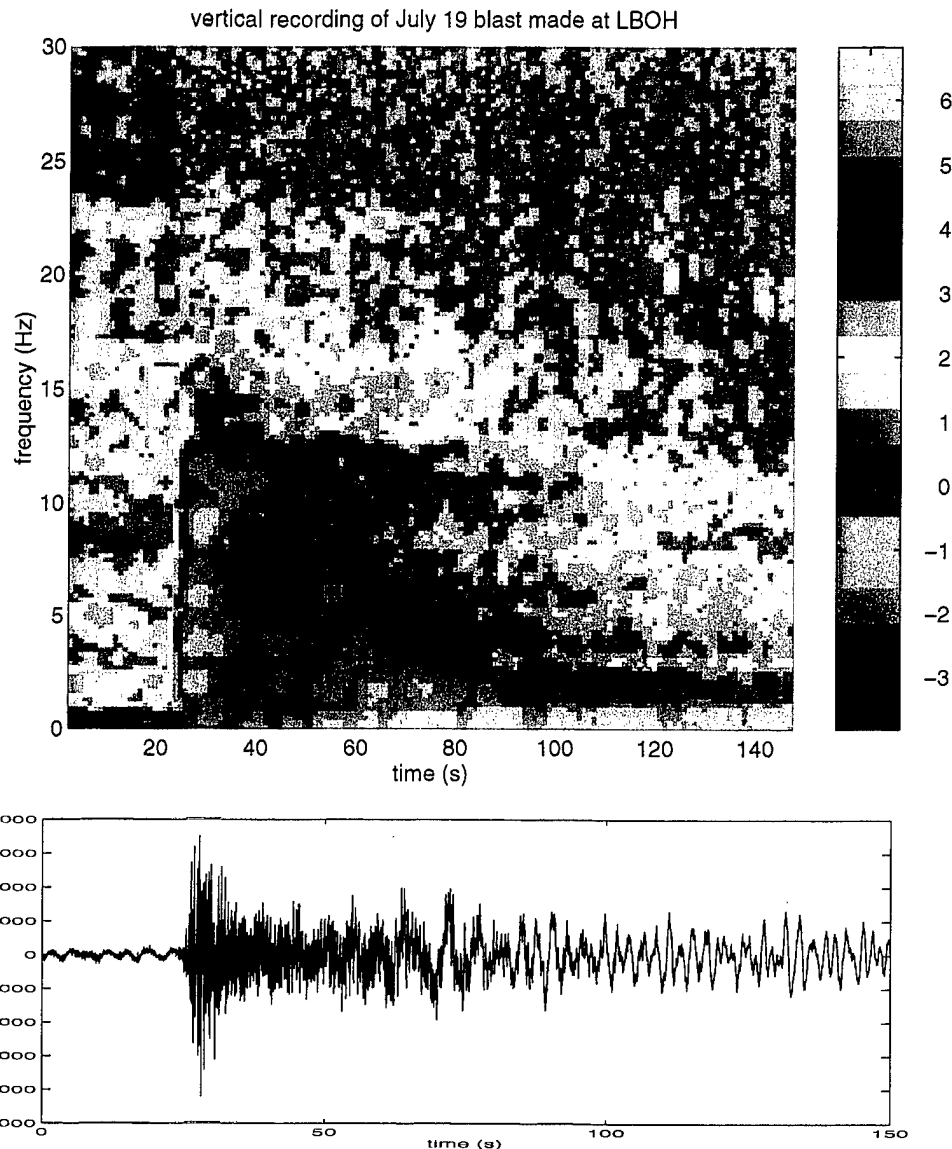


**Figure 9c.** Broadband sonogram and timeseries recorded by LBOH. The event was a 4.5 million pound cast shot detonated in the Black Thunder coal mine on July 19, 1996. Despite using millisecond delays, the shot did not generate obvious scallops at high frequency. Local recordings (made by LANL) indicate a weak, broad scallop at  $\sim 30$  Hz which is expected from this type of event (which employs 35 msec. intershot delays). This scallop did not survive propagation to this station (located 200 km to the west of the mine).

9c). This large (2.25 kT) event is a solid example of known millisecond delay-firing not yielding the expected modulations. It did not have a sympathetic component and was recorded at near-regional range with high signal-to-noise ratio. Attenuation is clearly a factor. Local recordings of Black Thunder cast shots (by LANL) reveal a weak, broad, spectral high at  $\sim 30$  Hz (the frequency of the fundamental interference mode produced by 35 msec delays). This scallop did not survive to 200 km, as signal falls into noise by  $\sim 25$  Hz at this range. The weakening of the scallop is easily synthesized by adding random perturbations to the shot times and, as discussed in the previous section, by allowing waveform variability (*Baumgardt, 1996*).

### **2.3 A Detonation Anomaly**

A second Black Thunder cast blast detonated with a significant sympathetic component (in which a large percentage of the total explosives detonated simultaneously; Figure 9d). As expected, this significantly boosted seismic body wave amplitudes (Figure 9e) and resulted in a body wave magnitude of 4.0. Signal onsets for the August 1 blast are unusual (Figure 9f). A clear pulse can be seen in II recordings at ~1.75 seconds after P wave onset. This event provides an empirical example of what might be expected from a "hide in quarry blast" evasive test. The event suggests that it would be difficult to hide a significant release of energy within a quarry blast because delay-firing spreads energy over time and yields weak body waves (see Section 4 for more). No conclusion can be made yet about how much energy can be hidden in this kind of event since the explosive yield of the simultaneous detonation is still unknown.

### **2.4 Analyses.**

The next 3 sections describe several analyses of the ground truth data that are complete or currently in progress.

### **Acknowledgments**

The Wyoming data would not have been collected without funding and equipment provided by Brian Stump, Craig Pearson and Rod Whitaker at LANL (under contracts 1973USML6-8F and F5310-0017-8F). Further support was provided by Robert Martin and David Gross at the Black Thunder coal mine and Vindell Hsu (AFTAC). Adam Edelman (IGPP) consistently was at the center of the solution to any problem encountered in the execution of the 1996 Wyoming field experiment. Further essential support and equipment was provided by Frank Vernon, the IGPP north lab and the IRIS PASSCAL program. The temporary seismic stations were made possible by Wenzel Kovarik, Reuben and Ruth Schreiner, Richard Kretschman, Bill Bartlett (BLM) and rangers in the Custer National Forest.

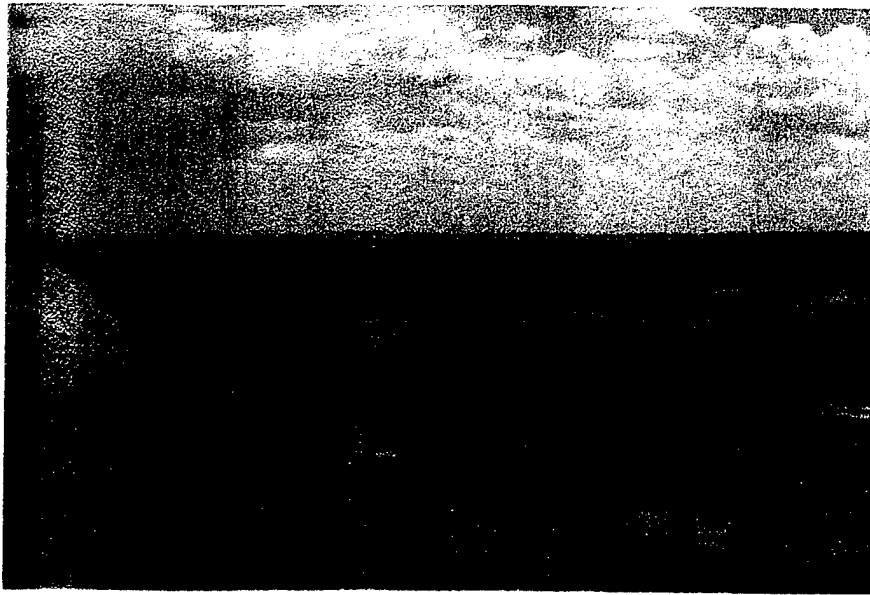


**Figure 9d.** Three photos of the August 1, 1996 Black Thunder cast blast. The start at 19:33:05 (top), 1.7 seconds later (middle) and the finale at 19:33:09. The significant release of energy into the air resulted from a sympathetic detonation which occurred part way through the shot sequence.

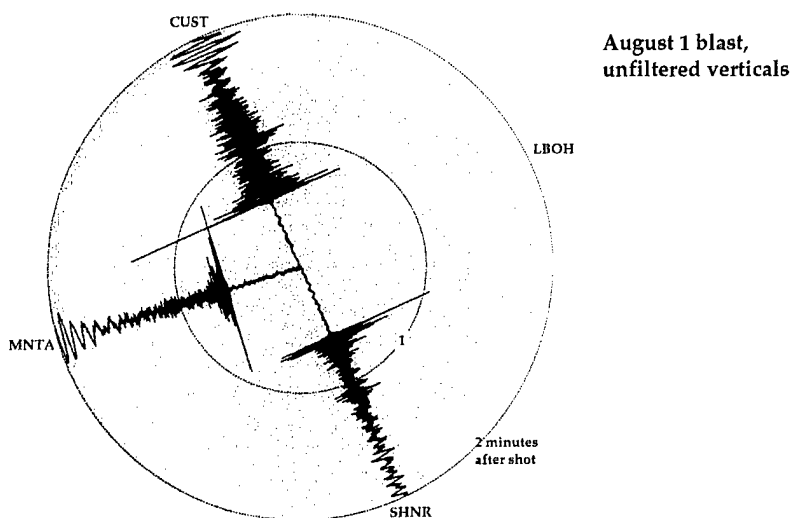
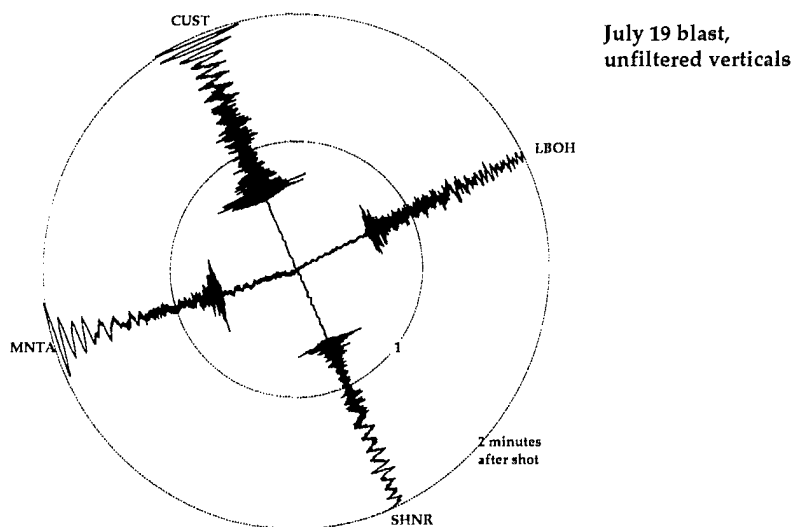


**Figure 9e.** Normalized seismograms from the azimuthal network. The July 19, 1996 blast (upper) used 4.5 million pounds of ANFO which detonated as planned. The lower (2.5 million pound shot; Aug 1, 1996) included a sympathetic component (details as yet unknown) which significantly boosted seismic body wave amplitudes but not the surface waves. LBOH was offline at the time of the second blast.

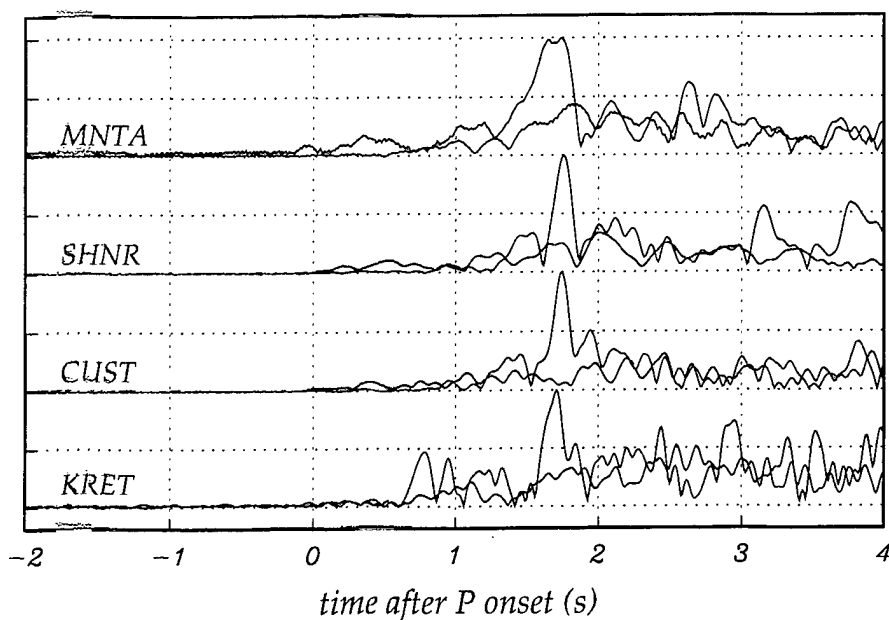


**Figure 9f.** Envelopes of unfiltered recordings made by the azimuthal network. The July 19.96 cast blast (black) is unlike the Aug 1.96 cast blast (red). A sharp pulse appears in each recording of the later event at  $\sim 1.75$  s after P wave onset.



### 3. Some Observations of Low Frequency Spectral Modulations

Although the previous section discusses spectral modulations which result from intershot delays, typical delay-fired mining events are exceedingly complex and provide other sources of scalloping. In cast explosions, for example used in coal mines in eastern Wyoming where overburden is moved or cast to expose the coal seam, there is significant spall (*Stump, 1995*). Each sub-shot in a cast source is followed by a series of significant impacts of casted material on the floor of the pit. The pairing of each sub-shot with a series of impacts delayed by roughly the same interval might produce a simple scalloping with a frequency spacing that is the inverse of the time delay. Regardless of how much explosives the miners have at their disposal, the delay-fired event will have a start and end - typically within a few seconds of each other. This temporal finiteness will also produce modulations (*Hedlin et al., 1990*) and sometimes a prominent spectral notch (*Gitterman and van Eck, 1993*). As with intershot delays, these temporal features (casting impact delay, source finiteness) should not depend on the orientation of the sensor.

#### 3.1 Time-independent Scallops Below 10 Hz.

This section reports observations of low frequency modulations recorded in Wyoming during the 1996 and 1997 collaborative field experiments. Two key elements of the two regional experiments were that broadband STS2 seismometers were used. These give a flat response between 0.0083 and 40 Hz and thus an opportunity to examine both the high and low frequency components of the regional wavefield. The seismometers recorded signals produced by delay fired coal and cast shots at mines in the Powder River Basin, as well as calibration shots detonated in the Black Thunder coal mine (Figure 9b). The calibration shots were detonated primarily so that the coal miners could assess the effect of cast shooting on local assets; however, they were recorded at regional distance above noise and can be used as proxies for nuclear tests.

Considering the likely impact of source finiteness on low frequencies, STFT's were calculated using long (15 s) windows. Averaged log spectra from the full network (Figures 10 - 12) show clear time-independent modulations which do not depend strongly on source-receiver azimuth and recording component. The blast reports can be used to predict spectral modulation, although as pointed out by *Stump et al. (1994)*, this kind of calculation is only useful as a rough guide since no blast will detonate exactly as planned. Although the planned July 19 shot spanned ~ 3.5 s, the bulk of the energy was expended in the middle 2 s. This leads to spectral modulations spaced ~ every 0.5 Hz - very similar to those observed in the spectra. Relatively significant modulations are expected every 2 Hz (with the most noticable one at 4 Hz). This prediction is, again, in rough agreement with what is observed in the spectra displayed in Figure 10. The modulations do, however, depend on the source type. The calibration shots (blue curves in Figure 10) did not yield coherent spectral modulations.

*July 19.96 cast vs 16,000 lb calib. shot*

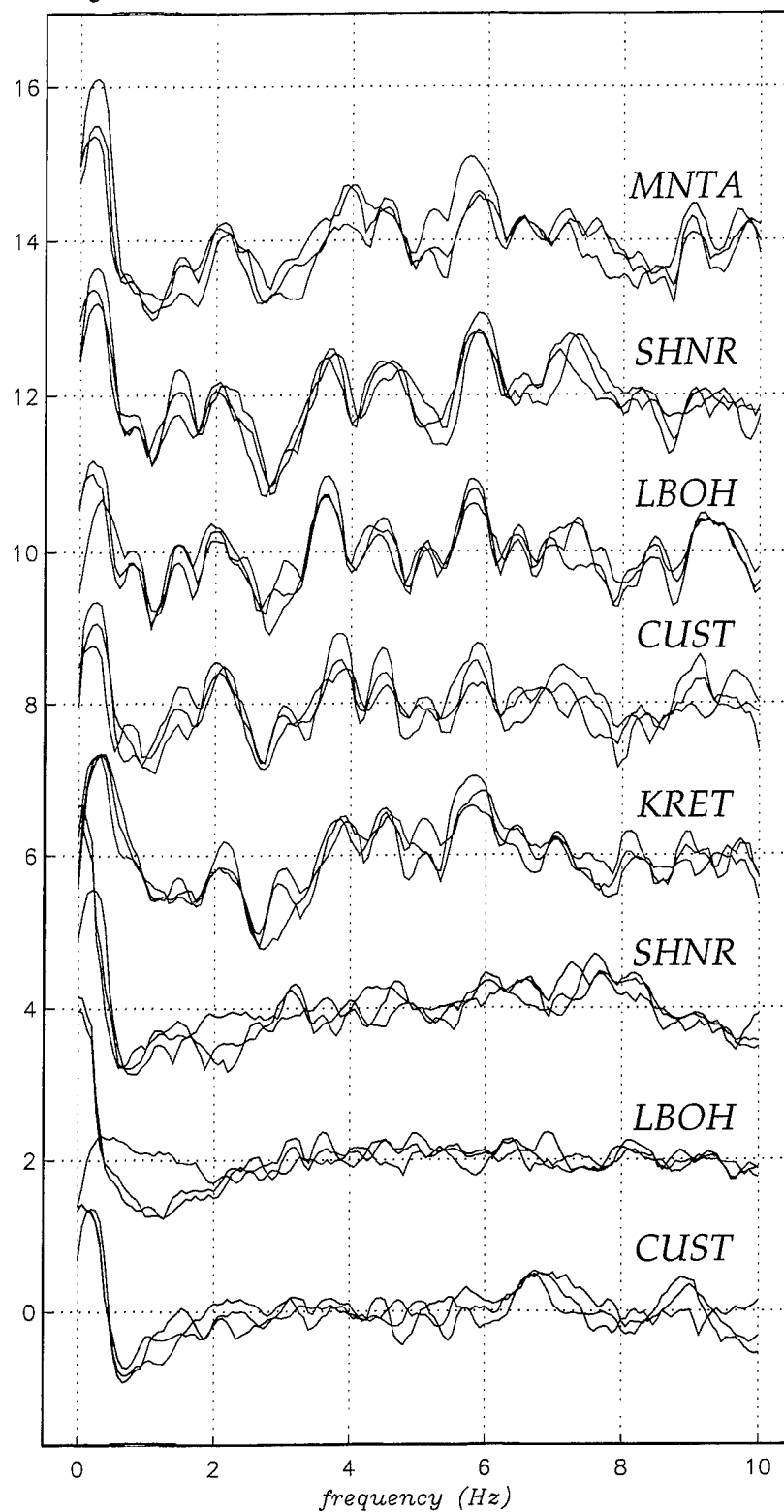


**Figure 10.** Although the broadband modulations are barely discernable, obvious time-independent modulations exist below 10 Hz. These are likely due to source finiteness and are largely independent of the recording direction. Each curve shown above represents the average of 46 estimates taken from staggered 15 s. windows which span 125 of P and S coda. Each 3C station yields 3 estimates.

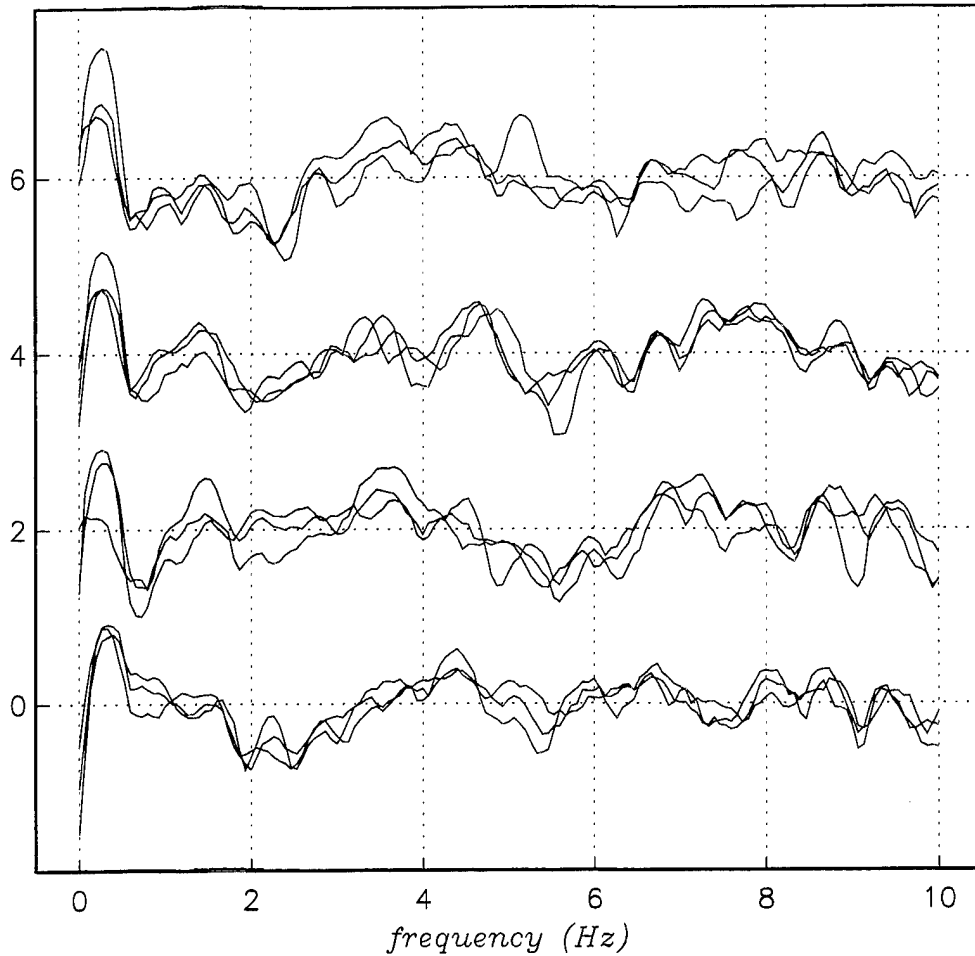


**Figure 11.** Low frequency spectral modulations produced by the August 1, 1996 cast blast (Figure 9a.).

The existence of low frequency modulations in the spectra of well documented (known millisecond delay-fired) cast shots in Wyoming is encouraging since these would be relatively resistant to attenuation and should be usable at a greater range. This example not only offers a possible remedy to the high-frequency problem, but is a reminder that the sonogram approach (discussed in the first section) must be regionally trained. All of the six datasets considered in the first section were analyzed using exactly the same input parameters (reviewed in the appendix). Perhaps the misclassification probabilities could have been improved by adapting these parameters to better accommodate local conditions. In Wyoming, the required tuning could be described better as a major overhaul - in regions where extensive cast shooting is the norm, the useful spectral features seem to lie below 10 Hz.

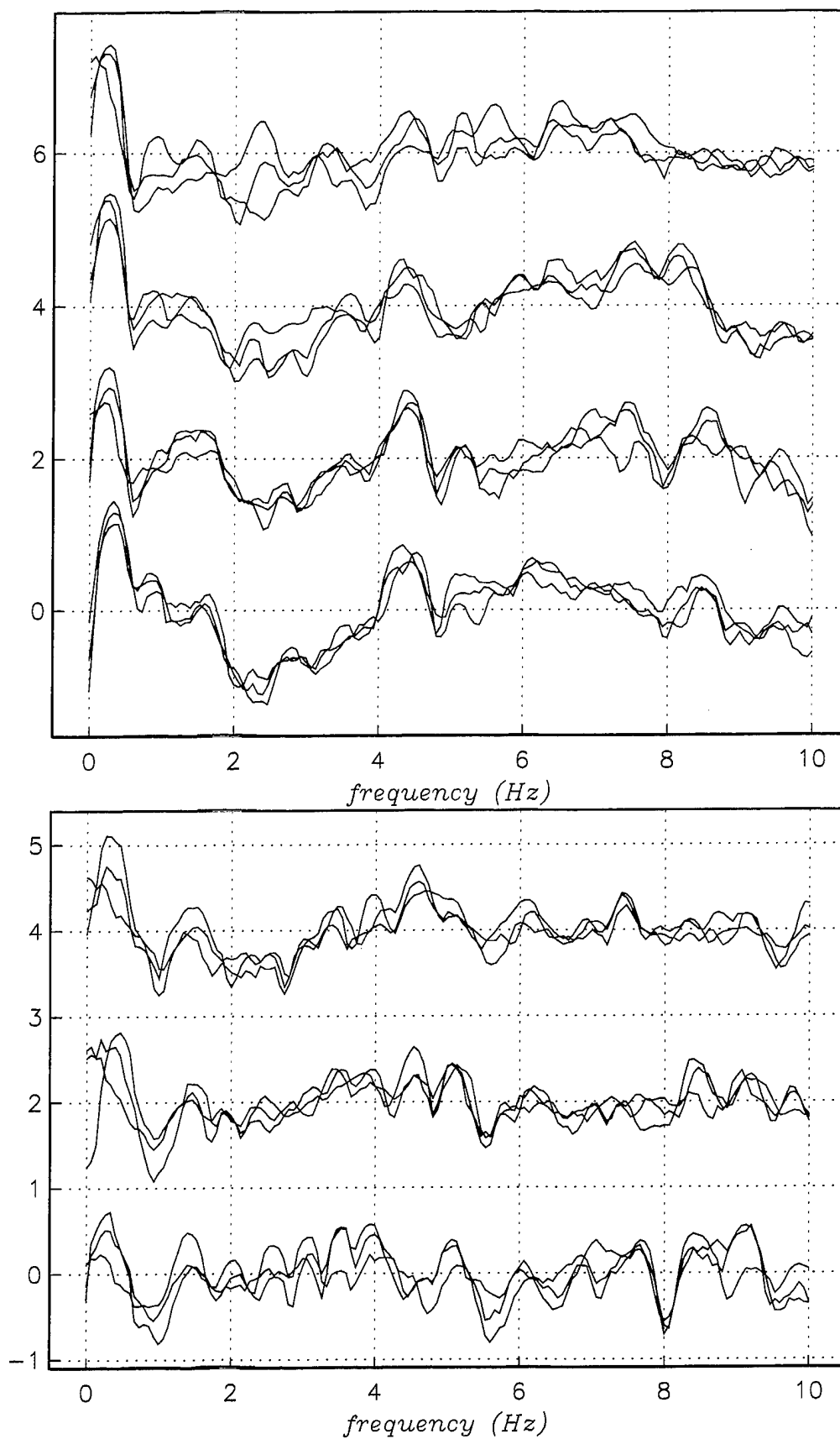


**Figure 12.** Spectral modulations produced by the Aug 2, 1996 and Aug 14, 1997 cast blasts (Figure 9a).

### 3.2 Current Work.

Clearly, this empirical observation needs to be placed on a firmer physical basis. Our upcoming work, funded by DSWA, will investigate the origin of these spectral modulations through physical modeling. The Wyoming experiments in 1996 and 1997 recorded well over 100 significant mine blasts in the Powder River Basin. The physical modeling will be accompanied by a thorough review of these recordings. The data will be used to determine the robustness of these features and if they are just a property of the largest cast shots or are produced by the smaller coal fragmentation blasts. If these modulations prove to be robust, a statistical test will be developed to detect them and discriminate mining blasts from instantaneous explosions.

## 4. Regional Observations of Time-domain Seismic Source Characteristics

### 4.1 A Regional "Ms:mb"

TTBT monitoring at teleseismic distances took advantage of significant surface and body waves emitted by large underground tests and earthquakes. One of the paramount discriminants from that era compared the relative strengths of the two types of energy. Recent work by *Anandakrishnan et al. (1997)* suggests that a similar approach might be used at regional distances to discriminate mining blasts from instantaneous explosions. They reported observations of significant long-period surface waves radiated by temporally and spatially extensive mine blasts. Unless the mine blast shot sequence detonates anomalously (*e.g.* with a significant proportion of the shots detonating sympathetically), these shots will excite body waves with low amplitudes.

### 4.2 An Obvious Mismatch Between Calibration and Cast Shots.

As mentioned in the second section of this report, the azimuthal seismic network (Figure 9a) recorded significant cast blasts occurring in the Powder River Basin and calibration shots detonated in the Black Thunder coal mine. The largest calibration test detonated 16,000 pounds of explosives. As shown in Figure 13, the body wave amplitudes of a 16,000 pound calibration shot rival those produced by a 4.5 million pound south pit cast blast (detonated without significant anomalies). As expected, the calibration shot was an insignificant source of surface waves (Figures 13 and 14).

These features are not unique to these two events but appear to be robust. In Figure 15 we compare the relative amplitudes of body and surface waves for 2 calibration and 4 cast shots. The August 1, 1996 cast blast detonated with a significant sympathetic component, giving significantly boosted body wave amplitude but undiminished surface waves.

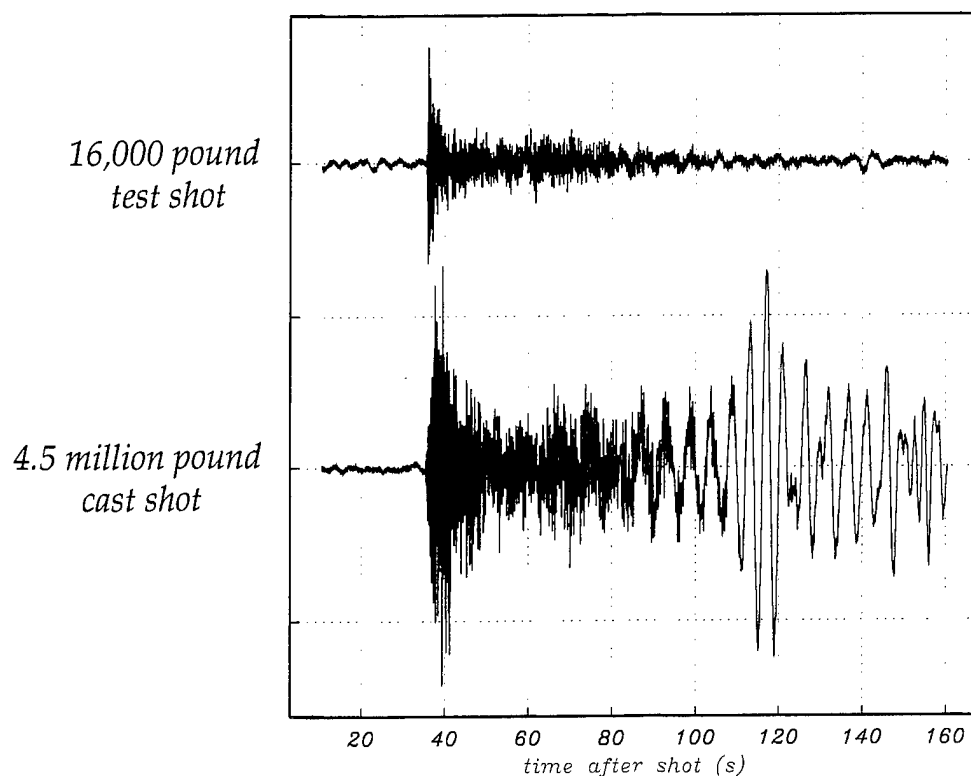


**Figure 13.** Unfiltered vertical component recordings of a 16000 pound calibration shot (top) and a 4.5 million pound cast shot made at CUST. The station was located 200 km to the north of the events (Figure 9a) which both occurred in the Black Thunder coal mine. The tiny calibration shot rivals the immense cast shot in P waves, but is an insignificant source of surface waves. The dissimilarity of unfiltered vertical component recordings made at CUST is not surprising (Kim *et al.*, 1994; Anandakrishnan *et al.*, 1997) and suggests that a regional version of the Ms:mb discriminant could be effective for separating large mine blasts from instantaneous explosions.

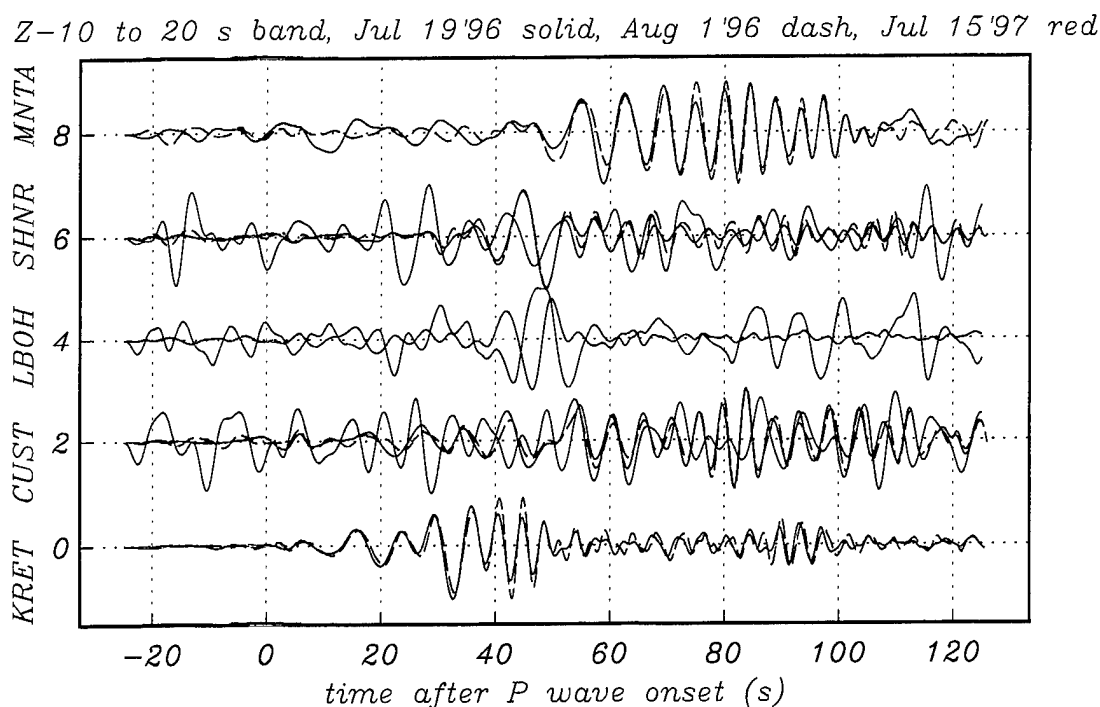


**Figure 14.** Long period calibration shot (red) and cast blast (black) waveforms. The calibration shot yielded little if any low frequency energy above noise in this band. In this example all traces are normalized to one.

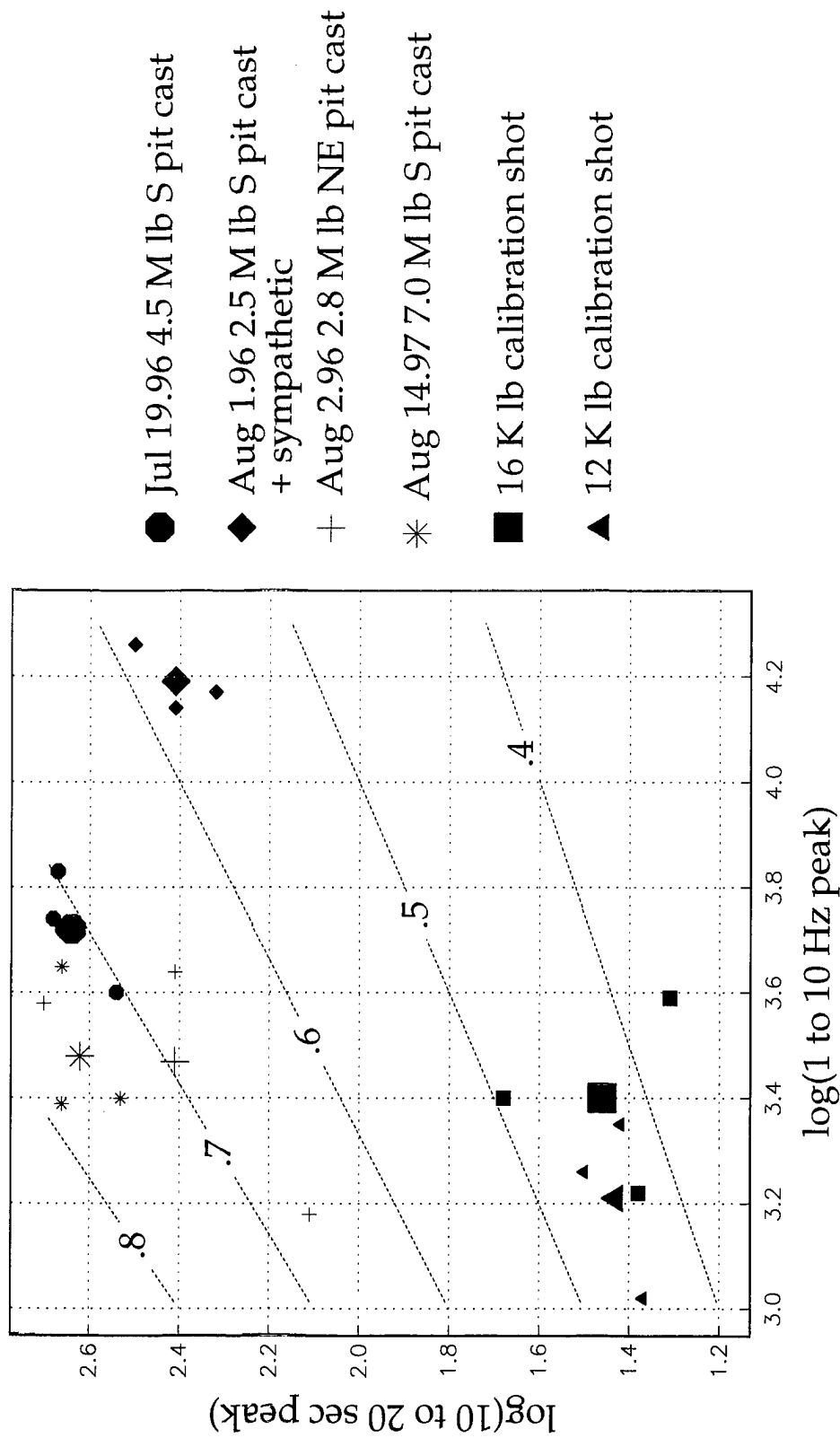


**Figure 15.** A comparison of 10 to 20 second surface wave and 1 to 10 Hz P wave peak amplitudes using recordings made at a range of 200 km by MNTA, CUST, LBOH & SHNR (see Figure 9a). All events occurred in the Black Thunder coal mine. Each trace is filtered, converted to an envelope and adjusted downward by an amount determined by pre-onset noise. Above are displayed the logarithms of the individual station peak amplitudes. The large symbols represent the network average for each event. Each labeled curve indicates a constant ratio of surface wave to P wave amplitude [*i.e.*  $\log(10 \text{ to } 20 \text{ s peak}) / \log(1 \text{ to } 10 \text{ Hz peak})$ ]. As expected, the calibration shots yield little surface wave energy above noise. The Aug 1 1996 cast shot appears to be somewhat explosion-like due to the sympathetic detonation (Figures 9d and 9e). The sympathetic detonation greatly boosted P wave amplitudes but left the surface waves untouched. Unadjusted amplitudes are at the same range from the mine.

### 4.3 Current Work

Although the data collected in Wyoming suggests regional Ms:mb can become a very effective discriminant, much work remains. The two experiments in Wyoming yielded recordings of numerous cast and smaller coal shots detonated in Black Thunder and neighboring coal mines. An upcoming analysis of these data should indicate if this discriminant is just effective for the largest cast blasts or will be useful for smaller blasts which do not have long source duration and cast significant mass of rock. Modeling (of the sort described by *Barker et al, 1993* and *Anandakrishnan et al., 1997*) will be used to place this method on a firmer physical basis.

### 4.4 Waveform correlation

Due to promising results reported in previous papers (*incl. Harris, 1991 and Riviere-Barbier & Grant, 1993*) regarding the use of waveform correlations for event characterization, we examine the seismic waveforms of 4 significant Black Thunder cast blasts. We have opted to look at 10 to 20 second period waves because of the observations made by *Anandakrishnan et al. (1997)* and because low frequencies are relatively immune to attenuation and should be usable for source characterization at a greater range. The azimuthal network (Figure 9a) has given us an opportunity to examine the dependence of these waveforms on azimuth. In addition, the Black thunder mine (Figure 9b) is very extensive and contains several mine pits. We have used the data to determine the dependence of the low frequency waveforms on the exact location of the shot and blasting parameters.

In Figure 16, we display low-passed waveforms from three Black Thunder south pit cast blasts (Figure 9b). The waveforms display a remarkable degree of independence from shot size (2.5 to 7 million pounds) and exact location in south pit (all located at the west end of the pit; approx. locations given in Figure 9b). All three of these shots were fired from east-to-west and south from the pit face, and material was thrown to the north. A large percentage of the ANFO in the smallest shot (green traces in Figure 16) detonated simultaneously. Although this sympathetic blast boosted body wave amplitudes, it has not affected the surface waves (Figure 9e). Although physical modeling is not complete, this observation suggests that once the source duration or spatial extent exceeds some threshold, significant surface waves will be generated. The source duration can then increase without further obvious effect on the temporal character of the surface waves (which seem to be highly dependent on the path and/or direction of the shooting/casting relative to the path to the station).

In Figure 16, we also show a comparison of a south pit blast with one detonated in the northeast pit (Figure 9b). In this case there exist notable differences between the two sets of waveforms, suggesting a need for separate "fingerprint" waveforms for these mine pits. Considering the results above, the only significant difference between these two shots was the exact location of the pit and the direction of shooting (Figure 9b shows the orientation of the NE pit relative to the south pit).



Z-10 to 20 s band, Jul 19'96 blue, Aug 1'96 green, Jul 14'97 red

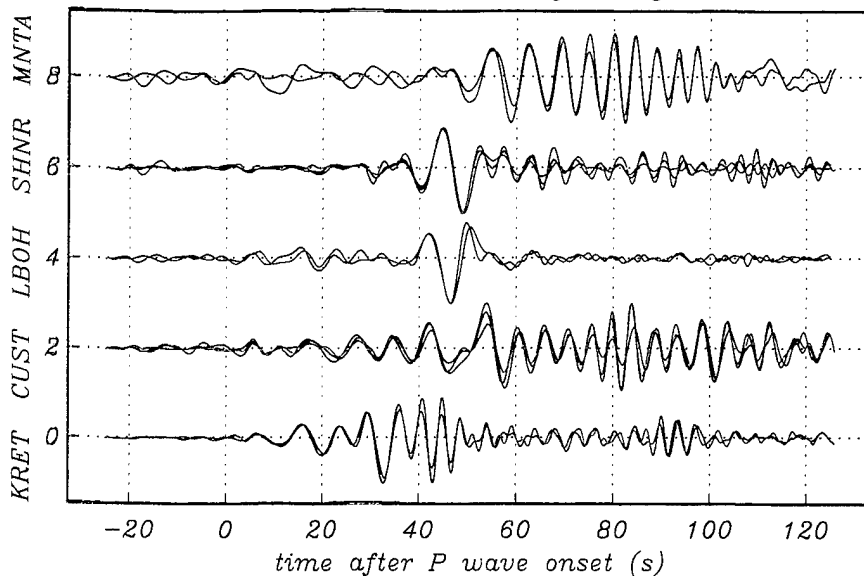
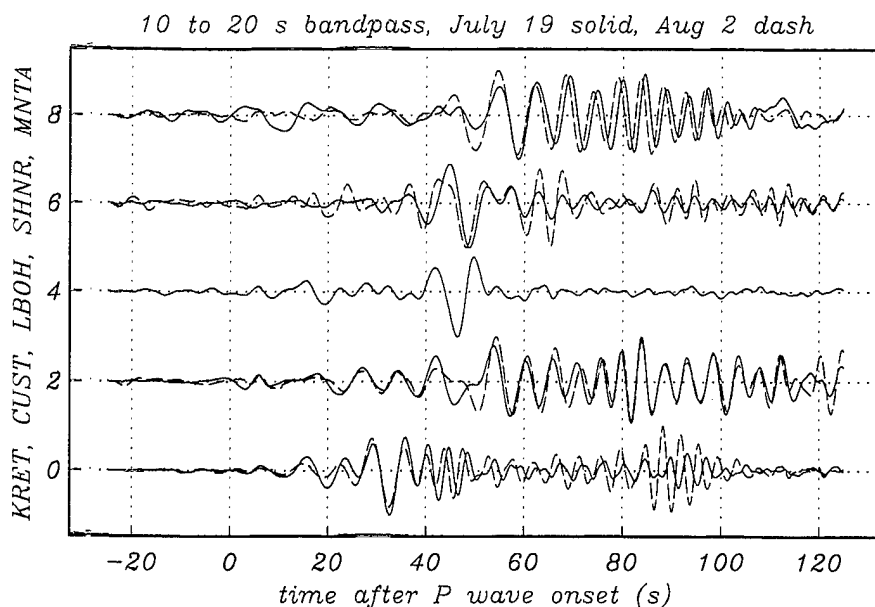


**Figure 16. (top)** A comparison of broadband regional seismograms from three different cast blasts at five different stations at varying azimuths from the mine (the azimuthal network displayed in Figure 9a). All shots were detonated in the south pit of the Black Thunder coal mine (Figure 9b). Low frequency seismic signals from the south pit events are remarkably robust although highly dependent on azimuth. **(bottom)** South pit (Jul 19, 1996) vs the Northeast pit (Aug2, 1996). There are obvious differences between the two sets of waveforms.



#### 4.5 Current Work on Waveform Correlation.

These observations are preliminary as a more thorough analysis, using physical modeling, has just begun. The utility of low frequency waveforms for regional source identification will be tested more thoroughly through an analysis of the 1996 and 1997 datasets.

## 5. Regional Acoustic Monitoring

In the 1950's and 1960's, there was considerable interest in infrasonic energy produced by atmospheric nuclear tests. With the advent of the LTBT in 1963, testing moved underground and seismic became the principal monitoring tool. Because of the CTBT, and concomitant interest in small and shallow events, infrasound has re-emerged as an important monitoring tool. Since natural or man-made events might emit energy into the atmosphere and into the Earth, and since each kind of energy comes with limitations, there is considerable interest in considering infrasonic and seismic signals together. *Sorrells et al. (1997)* have shown the utility of the two data sets in a study of mining explosions in northern Mexico, southeastern Arizona and southwestern New Mexico.

Under the CTBT, location and depth remain paramount indicators of event type. Although strong, shallow, earthquakes can produce a piston-like ground displacement and excite infrasonic waves in the atmosphere (*Blanc, 1989*), these events are much more efficient sources of seismic energy. A recent study (*Calais et al, 1997*) found acoustic ionospheric perturbations resulting from a magnitude  $\sim 3$  mine blast comparable to those produced by the magnitude 6.7 Northridge earthquake. The relative strength of acoustic and seismic signals might provide an effective depth discriminant.

Infrasound signals might further complement seismic by permitting a precise back azimuth estimate and thus giving a more certain event location.

### 5.1 1996 Infrasound Experiment

To test the utility of infrasound for regional monitoring, and as a tool to complement seismic discriminants such as the time-frequency method discussed in the first section, as part of the 1996 regional monitoring experiment a 3-element infrasound array was deployed 200 km to the west of the Powder River Basin with a STS-2 seismometer at MNTA (Figures 9a and 17). The array recorded highly coherent acoustic signals from the July 19, 1996 Black Thunder cast blast (Figure 18). An f-k analysis of the onset energy (Figure 19) returns a back-azimuth estimate within 1.75 degrees of the true mine azimuth. The signal remains close to this azimuth for 6 seconds, while signal levels remain strong.

### 5.2 A Simulation of the Effect of Wind Shear

In spite of this promising result, it is well known that propagation complexities hamper acoustic source studies. As shown in Figure 19, in the first 6 seconds after the onset of the acoustic signal from a mining blast there is an eastward bias in the back azimuth estimates. Although the bias at onset is very small, later bias ranges from 1 to 8 degrees, while the signal is strong, but increases to 15 degrees in the lull between arrivals. The error was likely due to wind shear since, at the time of the shot, high altitude (30 km) winds were strong ( $>30$  m/s) and directed almost due west between the source and receiver (Figure 20).

## *The Moneta Seismo/Acoustic Station*

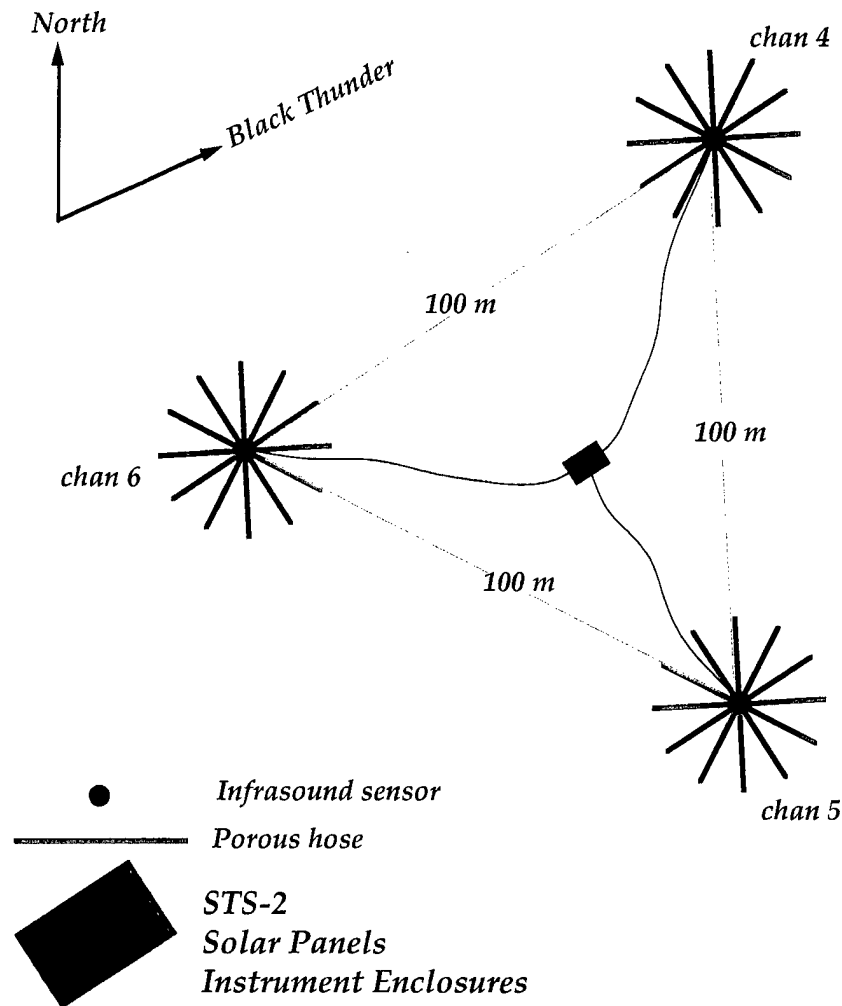


**Figure 17.** The layout of the infrasound array deployed at MNTA (Figure 9a). The array as co-located with a STS-2 broadband seismometer.

Wind shear will affect signal arrival direction and will have a significant impact on the strength of the refracted energy and the location at which the refraction caustic first returns to the ground. To estimate the effect of wind shear we simulated the propagation of 1 Hz energy using the Parabolic Equation method (Collins *et al.*, 1995). Two acoustic velocity models were used. The standard acoustic velocity profile (Calais *et al.*, 1997) was used to simulate propagation through calm atmosphere. To approximate wind shear we altered the standard atmospheric velocity at each altitude by adding an assumed wind speed (assumed to be horizontal and increasing from 0 at the free-surface by 1 m/s per km of altitude). Downwind energy is more highly focused and directed back to the earth at a shorter range (Figure 21).

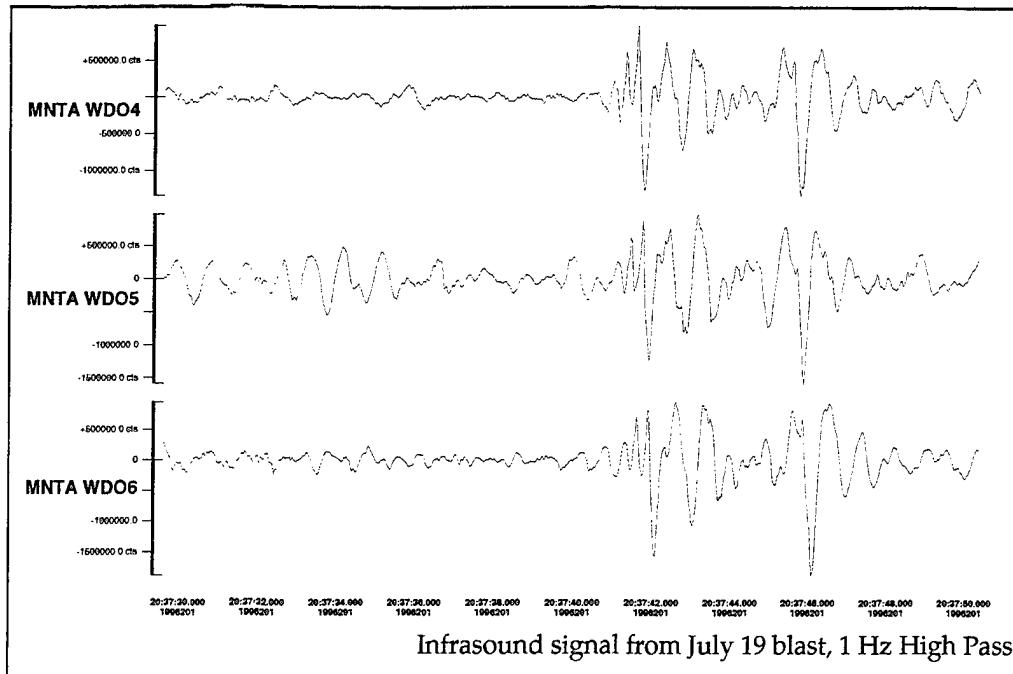


**Figure 18.** High-passed array recording of the signal from the July 19, 1996 4.5 million pound cast blast which occurred in the Black Thunder coal mine.

### 5.3 Recommendations.

Much work needs to be done to assess the value of acoustic data for small-event identification and to make the most of whatever synergy exists between acoustic and seismic signals. Although significant advances in the simulation of acoustic energy through a dynamic medium have been made (*e.g.* Collins et al., 1995), much work remains to be done on the quantification of the bias in signal strength and arrival direction caused by wind shear. We need to better understand what kinds of small man-made and natural events produce significant acoustic signals and how much of the source signature survives propagation through a dynamic atmosphere. Simulation experiments and source observations should accompany basic research into background infrasound noise levels and improvements in sensor and array design.

**Acknowledgements:** This experiment would not have occurred without the advice and logistical support provided by Rod Whitaker at LANL.

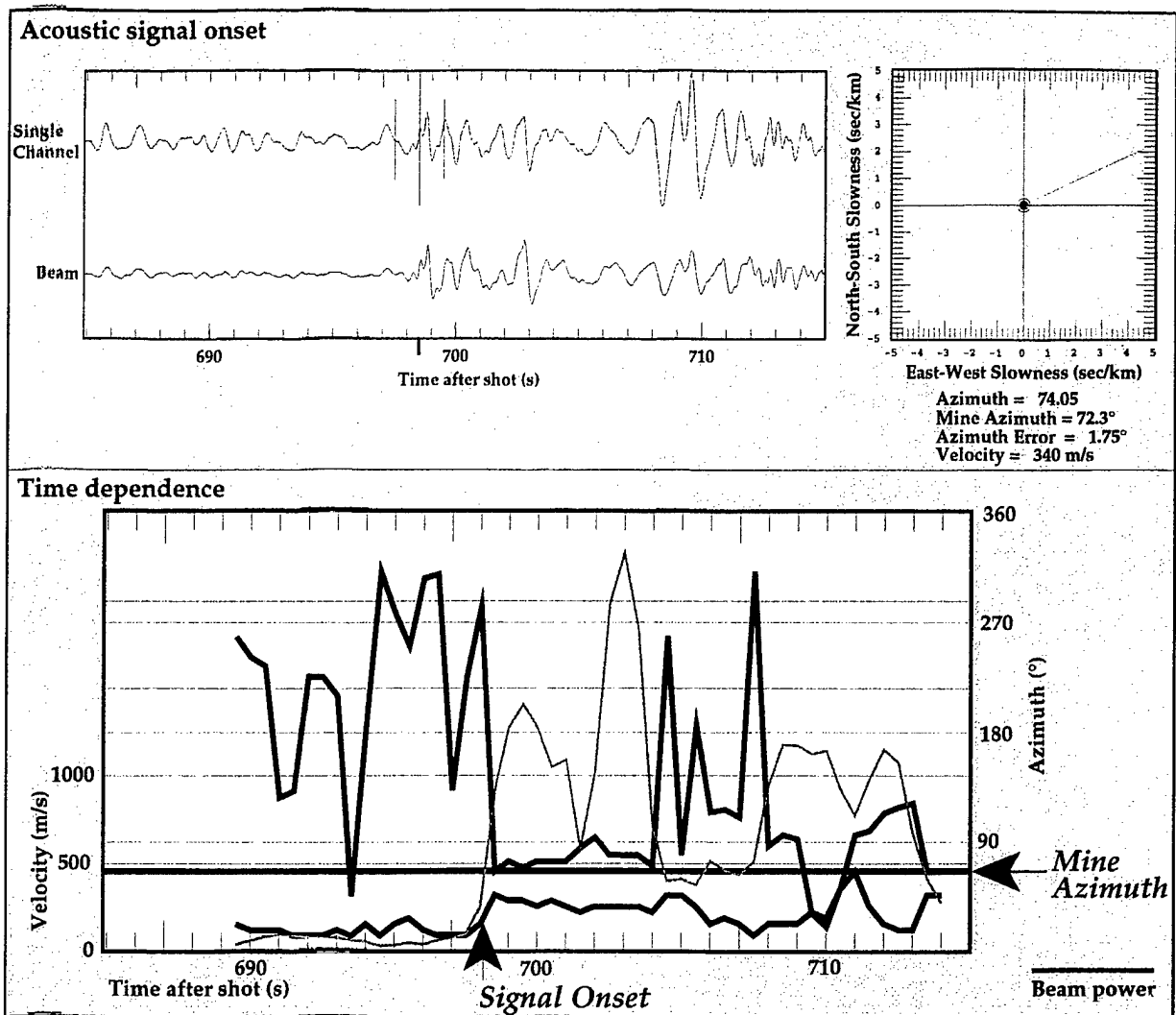


**Figure 19.** Acoustic data (upper traces) from the MNTA infrasound array. A single f-k estimate is shown in the upper right corner, while azimuth, velocity and signal power estimates are shown below.

## Wyoming region gridded wind speed data: July 19, 1996 at 1800 UTC

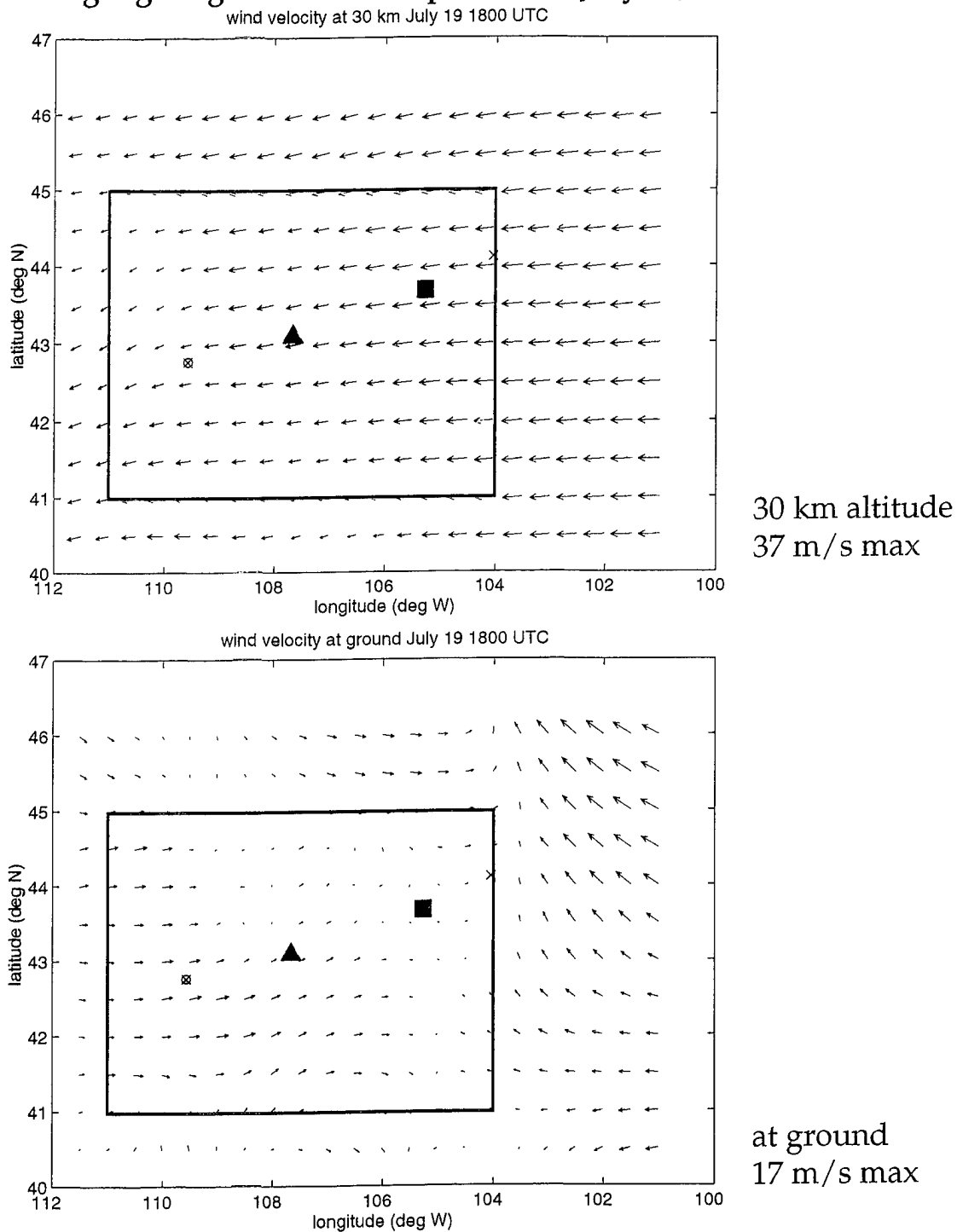


**Figure 20.** Gridded wind speed data for July 19, 1996 at the time of the cast blast. Wind is strong and directed due west at altitude while much weaker and highly variable at the surface. The outline of the state of Wyoming is given in red. The mine is represented by the solid square, the array is located at the triangle.

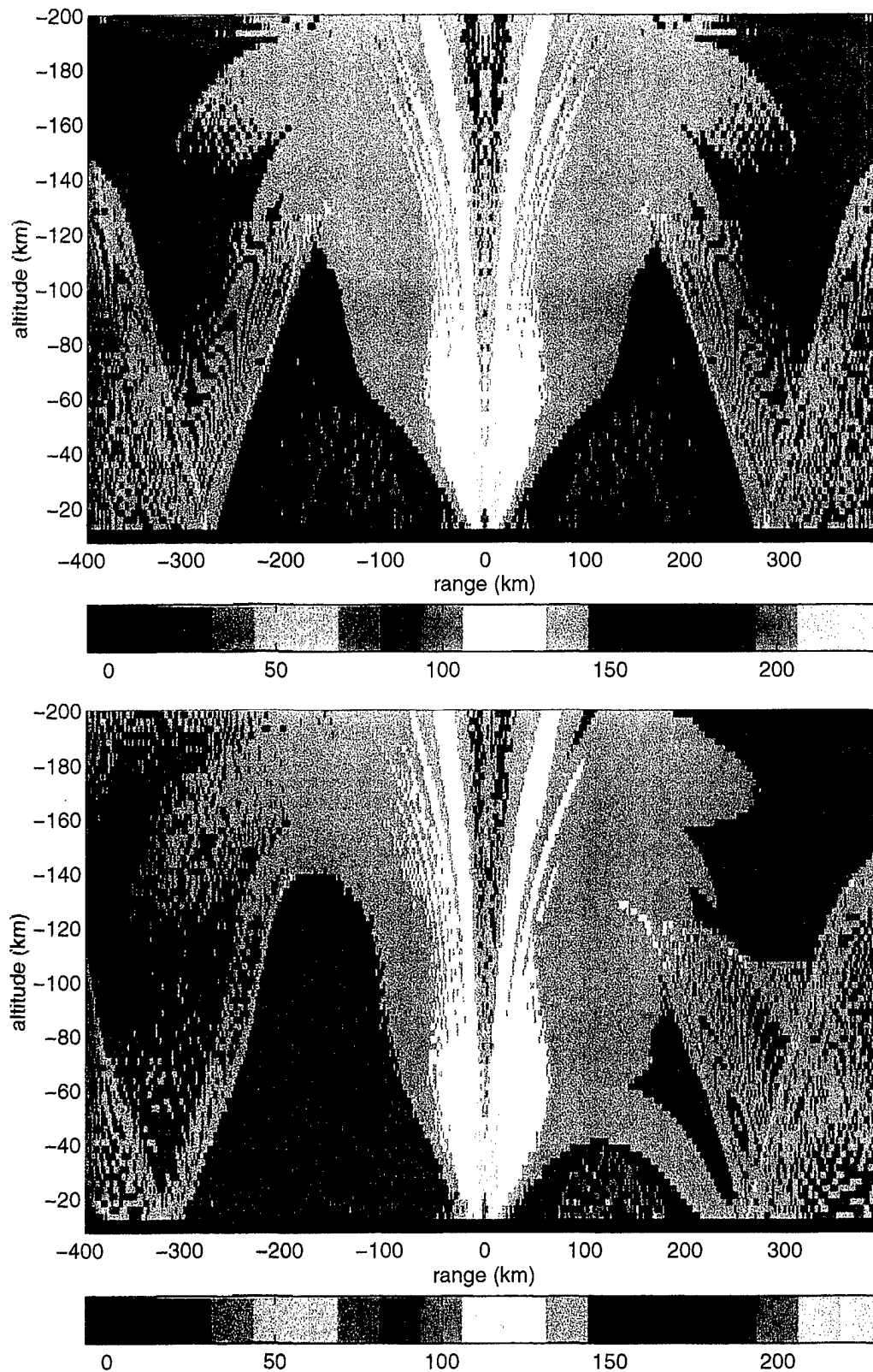


**Figure 21.** PE simulations of the propagation of 1 Hz acoustic energy through a stationary (top) and windy (bottom) atmosphere. For these simulations a standard atmosphere velocity model (*Calais et al., 1997*) was used. In the windy simulation the wind speed increased from 0 at the surface at a rate of 1 m/s for every 1 km of altitude and is directed from the left to right. Shading indicates transmission losses in dB.

#### 5.4 The 1996 Continuous GPS Experiment: Brief Overview of Results.

Although the results of this experiment and analysis are reviewed in detail in *Calais et al. (1997)*, a brief summary is given here. Sources such as atmospheric or buried explosions and shallow earthquakes are known to produce infrasonic pressure waves in the atmosphere. Because of the coupling between neutral particles and electrons at ionospheric altitudes, these acoustic and gravity waves induce variations of the ionospheric electron density. The Global Positioning System (GPS) provides a way of directly measuring the total electron content in the ionosphere and, therefore, of detecting such perturbations in the upper atmosphere. In July and August 1996, 3 large surface mine blasts (1.5 to 2.25 kT) were detonated at the Black Thunder coal mine in eastern Wyoming (Figure 9b). As part of a seismic and acoustic monitoring experiment, we deployed 5 dual-frequency GPS receivers at distances ranging from 50 to 200 km from the mine (Figure 9a) and were able to detect the ionospheric perturbation caused by the blasts. The perturbation starts 10 to 15 minutes after the blast, lasts for about 30 minutes and propagates with an apparent horizontal velocity of 1200 m/s. Its amplitude reaches  $3 \times 10^{14}$  el/m<sup>2</sup> in the 7-3 minutes period band, a value close to the ionospheric perturbation caused by the magnitude 6.7 Northridge earthquake (*Calais & Minster, 1995*). The small signal-to-noise ratio of the perturbation can be improved by slant-stacking the electron content time series recorded by the different GPS receivers taking into account the horizontal propagation of the perturbation. The energy of the perturbation is concentrated in the 200 to 300 s period band, a result consistent with previous observations and numerical model predictions. The 300 second band probably corresponds to gravity modes and shorter periods to acoustic modes, respectively. Using a one-dimensional stratified velocity model of the atmosphere, we show that linear acoustic ray tracing fits arrival times at all GPS receivers. We interpret the perturbation as a direct acoustic wave caused by the explosion itself. This study shows that even relatively small subsurface events can produce ionospheric perturbations that are above the detection threshold of the GPS technique.

#### 5.5 Implications for CTBT Monitoring

Currently, the CTBT calls for an International Monitoring System comprising a global network of 60 ground-based infrasound stations. Due to low-velocity sound channels located between the free-surface and about 100 km altitude, acoustic energy emitted by near-surface events is preferentially refracted back to the surface (Figure 21). Because of capricious wind speeds, the effective sound speed changes with time and the strength of the refraction caustic and the location where it first meets the ground is variable. Since current CTBT language calls for atmospheric acoustic monitoring to be conducted solely by ground-based infrasound sensors, the existence of this caustic has important ramifications for the use of acoustic energy for source detection, location and identification. An infrasound station located, by chance, just within the inner boundary of the first convergence zone could be close to the event (within 200 km) but likely not able to detect any significant signals. A station located at the caustic might detect a strong signal but, unless the wind is well known, might be unable to facilitate accurate source characterization. Consequently, a technique like continuous GPS, which is capable of



probing the upper atmosphere for derivative signals which can be sensed within a broad region including the first quiet zone, might be a good complement to infrasound monitoring. From a verification perspective ionospheric sensing is, as yet, an unevaluated technology. The present study suggests that dual-frequency GPS monitoring could potentially be very useful for CTBT verification.

## References

- Aviles, C. A. & Lee, W. H. K., 1986, Variations in Signal Characteristics of Small Quarry Blasts and Shallow Earthquakes, *EOS, Trans. of the American geophys Union*, **67**, 1093.
- Barker, T.G. & Day, S.M., 1990, A simple physical model for spall from nuclear explosions based upon two-dimensional nonlinear numerical simulations, PL-TR-90-0189, ADA231792.
- Barker, T.G., McLaughlin, K.L. & Stevens, J.L., 1993, Numerical imulation of quarry blast sources, Phillips Laboratory Technical report, SSS-TR-93-13859.
- Baumgardt, D.R., 1996, Case studies of seismic discrimination problems and regional discriminant transportability, PL final report PL-TR-95-2106, ADA302362.
- Baumgardt, D.R. & Young, G.B., 1990, Regional seismic waveform discriminants and case-based event identification using regional arrays, *Bull. Seism. Soc. Am.*, **80b**, 1874-1892.
- Baumgardt, D. R. & Ziegler, K. A., 1988, Spectral Evidence for Source Multiplicity in Explosions: Application to Regional Discrimination of Earthquakes and Explosions, *Bull. Seism. Soc. Am.*, **78**, 1773-1795.
- Baumgardt, D. R. & Ziegler, K. A., 1989, Automatic recognition of economic and underwater blasts using regional array data, Science Applications Incorporated, 11-880085-51
- Bell, A. G. R., 1977, A Digital Technique for Detection of Multiple Seismic Events, *EOS, Trans. of the American geophys. Union*, **57**, 444.
- Bennett, T.J., Barker, B.W., McLaughlin, K.L. & Murphy, J.R., 1989, Regional discrimination of quarry blasts, earthquakes and underground nuclear explosions, Final Report, GL-TR-89-0114, S-Cubed, La Jolla, California, ADA223148.
- Berger, J., Eissler, H.K., Vernon, F.L., Nersesov, I.L., Gokhberg, M.B., Stolyrov, O.A. and Tarasov, N.D., 1987, Studies of High-Frequency Seismic Noise in Eastern Kazakhstan, *Bull. Seism. Soc. Am.*, **78**, 1744-1758.
- Blanc, E., 1989, Observations in the upper atmosphere of ionospheric irregularities observed by HF soundings over a powerful acoustic source, *Radio Science*, **24**, 3, 279-288.
- Calais, E. & Minster, J.-B., 1995, GPS detection of ionospheric perturbations following the January 7, 1994, Northridge earthquake, *Geophys. Res. Lett.*, **22**, 1045-1048.
- Calais, E., Minster, J.B., Hofton, M. & Hedlin, M.A.H., 1997, Ionospheric signature of surface mine blasts from Global Positioning System measurements, *Geophysical Journal International*, in press.
- Carr, D. & Garbin, D., 1996, Discriminating ripple-fired explosions with high frequency (> 20 Hz) data, submitted to the *Bull. Seism. Soc. Am.*
- Chapman, M.C., Bollinger, G.A. & Sibol, M.S., Spectral studies of the elastic wave radiation from Appalachian earthquakes and explosions - explosion source spectra modeling using blaster's logs, *13th annual PL/DARPA Seismic Research Symposium*, 138-144, PL-TR-91-2208, ADA241325.
- Collins, M.D., McDonald, B.E., Kuperman, W.A. & Siegmann, W.L., 1995, Jovian acoustics and comet Shoemaker-Levy 9, *J. Acoust. Soc. Am.*, **97**, 2147-2158.
- Daubechies, I., 1990, The wavelet transform, time-frequency localization and signal analysis, *IEEE Transactions on information theory*, **36**, 961-1005.
- Daubechies, I., 1996, Where do wavelets come from?-A personal point of view, *Proceedings of the IEEE; Special Issue on Wavelets*, **84**, 510-513.
- Der, Z.A. & Baumgardt, D.R., 1994, Source diagnostics from spectral modulation patterns in regional recordings of seismic waves from quarry blasts, *EOS, Trans. of the American geophys. Union*, **75**, 428.
- Dysart, P.S. & Pulli, J.J., 1990, Regional seismic event classification at the NORESS array: seismological measurements and the use of trained neural networks, *Bull. Seism. Soc. Am.*, **80**, 1910-1933..
- Gitterman, Y. & van Eck, T., 1993, Spectra of quarry blasts and microearthquakes recorded at local distances in Israel, *Bull. Seism. Soc. Am.*, **83**, 1799-1812.
- Grant, L. & Carabajal, C., 1995, Ground-Truth Database for Regional Seismic Identification Research, *Proceedings of the 17th Seismic Research Symposium*, Scottsdale, AZ, Sept 12-15, PL-TR-95-2108, ADA310037.
- Harris, D.B., 1991, A waveform correlation method for identifying quarry explosions, *Bull. Seism. Soc. Am.*, **81**, 2395-2418.

- Hedlin, M.A.H., Minster, J.-B. & Orcutt, J.A., 1989, The time-frequency characteristics of quarry blasts and calibration explosions recorded in Kazakhstan, U.S.S.R., *Geophys. J. Int.*, **99**, 109-121.
- Hedlin, M.A.H., Minster, J.-B. & Orcutt, J.A., 1990, An automatic means to discriminate between earthquakes and quarry blasts, *Bull. Seism. Soc. Am.*, **80**, 2143-2160.
- Hedlin, M.A.H., Vernon, F.L., Minster, J.-B. & Orcutt, J.A., 1995, Regional Small-Event Identification using Seismic Networks and Arrays, *proceedings of the 17th Seismic Research Symposium on Monitoring a CTBT*, Scottsdale, AZ, Sept, p 875-884, PL-TR-95-2108, ADA310037.
- Kim, W.Y., Simpson, D.W. & Richards, P.G., 1993, Discrimination of earthquakes and explosions in the eastern United States using regional high-frequency data, *Geophysical Research Letters*, **20**, 1507-1510.
- Kim, W.Y., Simpson, D.W. & Richards, P.G., 1994, High-frequency spectra of regional phases from earthquakes and chemical explosions, *Bull. Seism. Soc. Am.*, **84**, 1365-1386.
- Kim, W.Y., Aharonian, V., Lerner-Lam, A.L. & Richards, P.G., 1997, Discrimination of earthquakes and explosions in southern Russia using regional high-frequency three-component data from the IRIS/JSP Caucasus network, *Bull. Seism. Soc. Am.* - in press.
- Lachenbruch, P.A. & Mickey, M.R., 1968, Estimation of error rates in discriminant analysis, *Technometrics*, **10**, 1-11.
- Leith, W., 1994, Large chemical explosions in the Former Soviet Union and blasting estimates for countries of nuclear proliferation concern, *Arms Control and Nonproliferation Technologies*, 1st quarter 1994, 25.
- Lilly, J. & Park, J., 1995, Multiwavelet spectral and polarization analyses of seismic records, *Geophysical Journal International*, **122**, 1001-1021.
- McLaughlin, K.L., Barker, T.G., Stevens, J.L. & Day, S.M., 1994, Numerical simulation of quarry blast sources, PL final report SSS-FR-94-14418.
- Mellors, R.J., Vernon, F.L., Pavlis, G.L., Abers, G.A., Hamburger, M.W., Ghose, S. & Iliasov, B., 1997, The Ms=7.3 1992 Suusamy, Kyrgyzstan, Earthquake: 1. Constraints on Fault Geometry and Source Parameters Based on Aftershocks and Body-Wave Modeling, *Bull. Seism. Soc. Am.*, **87**, 11-22.
- Minster, B. & Day, S., 1986, Decay of wavefields near an explosive source due to high-strain, nonlinear attenuation, *J. Geophys. Res.*, **91**, 2113-2122.
- Mykkeltveit, S., Astebol, K., Doornbos, D.J. & Husebye, E.S., 1983, Seismic array configuration optimization, *Bull. Seism. Soc. Am.*, **73**, 173-186.
- Park, J., Lindberg, C.R. & Vernon, F.L., Multitaper Spectral Analysis of High-Frequency Seismograms, *J. Geophys. Res.*, **92**, 12675-12684.
- Patton, H.J., 1993, Discrimination of low magnitudes: Summary of potential and recent results, *EOS, Trans. of the American geophys Union*, **74**, 58.
- Pearson, D.C., Stump, B.W., Baker, D.F. & Edwards, C.L., 1995, The LANL/LLNL/AFTAC Black Thunder Mine regional mining blast experiment, *Proceedings of the 17th Seismic Research Symposium on Monitoring a CTBT*, Scottsdale, AZ, Sept, p562-571, PL-TR-95-2108, ADA310037.
- Pomeroy, P.W., Best, W.J. & McEvilly, T.V., 1982, Test ban treaty verification with regional data - a review, *Bull. Seism. Soc. Am.*, **72**, S89-S129.
- Richards, P.G., Lerner-Lam, A., Such, R. & Simpson, D., 1989, Chemical explosions and the discrimination problem, *11th annual DARPA/AFGL Seismic Research Symposium*, 63-66. GL-TR-90-0301, ADA229228.
- Richards, P.G., Anderson, D.A. & Simpson, D.W., 1992, A survey of blasting activity in the United States, *Bull. Seism. Soc. Am.*, **82**, 1416-1433.
- Riviere-Barbier, F. & Grant, L.T., 1993, Identification and location of closely spaced mining events, *Bull. Seism. Soc. Am.*, **83**, 1527-1546.
- Sereno, T.J. & Orcutt, J.A., 1985, Synthetic seismogram modelling of the oceanic Pn Phase, *Nature*, **316**, 246-248.
- Seber, G.A.F., 1994, *Multivariate Observations*, Wiley series in probability and mathematical statistics, John Wiley & Sons, Inc.
- Shumway, R.H., 1996, Array detection of ripple-fired signals: the Cepstral F-statistic, *The Phillips Lab scientific report*, PL-TR-96-2253, ADA319833.
- Smith, A.T., 1989, High-frequency seismic observations and models of chemical explosions: Implications for the discrimination of ripple-fired mining blasts, *Bull. Seism. Soc. Am.*, **79**, 1089-1110.
- Sorrells, G.G., Herrin, E.T. & Bonner, J.L., 1997, Construction of regional ground truth databases using seismic and infrasonic data, *Seism. Res. Lett.*, **68**, 743-752.
- Stump, B.W., 1995, Practical observations of US mining practices and implications for CTBT monitoring, *Phillips Lab report*, PL-TR-95-2108, ADA310037.
- Stump, G.W., Riviere-Barbier, F., Chernoby, I. & Koch, K., 1994, Monitoring a test ban treaty presents scientific challenges, *EOS, Trans. of the American geophys. Union*, **75**, 265.
- Stump, B.W., Pearson, D.C., Edwards, C.L. & Baker, D.F., 1995, The LANL Source Geometry Experiment, *proceedings of*

- the 17th Seismic Research Symposium on Monitoring a CTBT, Scottsdale, AZ, Sept, p684-693, PL-TR-95-2108, ADA310037.
- Stump, B.W., Anderson, D.P. & Pearson, D.C., 1996, Physical constraints on mining explosions: Synergy of Seismic and Video data with 3D models, *Seismological Research Letters*, **67**, 9-24.
- Su, F., Aki, K. & Biswas, N.N., 1991, Discriminating quarry blasts from earthquakes using coda waves, *Bull. Seism. Soc. Am.*, **81**, 162-178.
- Suteau-Henson, A. & Bache, T.C., 1988, Spectral characteristics of regional phases recorded at NORESS, *Bull. Seism. Soc. Am.*, **78**, 708-725.
- Suteau-Henson, A., Israelsson, H., Ryaboy, V. & Ryall, A., 1989, Analysis of high-frequency data, *11th annual DARPA/AFGL Seismic Research Symposium*, 67-88, GL-TR-90-0301, ADA229228.
- Taylor, S.R., 1995, Problems associated with Pg/Lg ratios from NTS explosions affecting seismic discrimination, *LANL technical report*, LAUR-95-3635.
- Thomson, D.J., 1982, Spectrum Estimation and Harmonic Analysis, *IEEE Proc.*, **70**, 1055-1096.
- Thurber, C., Given, H. & Berger, J., 1989, Regional Seismic Event Location With a Sparse Network: Application to Eastern Kazakhstan, USSR, *Journal of Geophysical Research*, **94**, 17767-17780.
- Tribolet, J. M., 1979, Seismic Applications of Homomorphic Signal Processing, Prentice-Hall Signal Processing Series.
- Vernon, F.L., 1994, The Kyrgyz seismic network, *IRIS newsletter*, 7-8, XIII, 2.
- Vernon, F.L., Mellors, R.J., Berger, J., Al-Amri, A.M. & Zollweg, J., 1996, Initial Results from the Deployment of Broadband Seismometers in the Saudi Arabian Shield, *Proceedings of the 18th Seismic Research Symposium, Annapolis, MD, Sept 4-6*, PL-TR-96-2153, ADA313692.
- Wuster, J., 1993, Discrimination of chemical explosions and earthquakes in central Europe - a case study, *Bull. Seism. Soc. Am.*, **83**, 1184-1212.

## Appendix - The Automated Time-frequency Discriminant

We have noted (in the main body of this paper and previously in *Hedlin et al., 1989*) that the frequency content of seismic onsets and coda resulting from delay-fired explosions is often highly independent of the recording component and time. It is well known that the energy is often scalloped in frequency (*e.g. Bell, 1977; Baumgardt & Ziegler, 1988*). These qualities are due to source finiteness, the intershot delays or a combination of the two (*Hedlin et al., 1989; 1990*). They can sometimes be acquired during propagation through a resonant crust (*Hedlin et al., 1989*).

To determine the degree to which these qualities are present in a seismic coda we first expand the recording into a time-frequency display (sonogram) by sliding a window (usually 2.5 seconds long) along the time series (with the window sliding 20% of its length each time). A spectral estimate is calculated at each window position, typically using 7 multitapers (*Thomson, 1982; Park et al., 1987*) with a time-bandwidth product of 4. As described in *Hedlin et al. (1989)* each multitaper spectral estimate is converted into binary form through convolution with two boxcars (usually spanning 4.4 and 2.0 Hz), differencing the two smoothed spectra and replacing all locally high (and low) spectral values with +1 (and -1). Using the original, spectral sonogram we estimate the average pre-onset noise level,  $N(f)$ , and randomize all values in the binary sonogram,  $B(f,t)$ , which have a smaller amplitude than this average. This randomization is recorded by a mask,  $R(f,t)$ , which equals 1 or 0 (indicating a randomized point or one that is untouched). Noise suppression is directed at long-lived spectral lines which would, if left untouched, give a sonogram an improperly high level of time-independence. Although the sonograms contain a wealth of information about the evolution of spectral energy in seismic coda, they must be collapsed into a few parameters which are diagnostic of delay-firing and can be used for automatic source discrimination.

*Independence from recording direction.* This quality is estimated simply by calculating the zero lag cross-correlation between the three pairs of binary sonograms (vertical with east-west; vertical with north-south, north-south with east-west). Given two binary sonograms E and Z (obtained from the east-west and vertical recordings of the same event) the zero lag cross-correlation is given by:

$$X_{EZ} = \frac{\sum_{i=1}^{n_{freq}} \sum_{j=1}^{n_{time}} E(i,j)Z(i,j)R_E(i,j)R_Z(i,j)}{\sum_{i=1}^{n_{freq}} \sum_{j=1}^{n_{time}} R_E(i,j)R_Z(i,j)}$$

where  $R_E$  and  $R_Z$  are the east-west and vertical component randomization masks. This sum incorporates only those points which have not been randomized. The perfect correspondence of non-randomized points would yield a cross correlation of 1.0. We do not rotate the data into source-centric coordinates (vertical, radial and transverse), since this was found to yield no improvement - as discussed in section 2, it seems that strong spectral scalloping is present in the same form regardless of how the sensor is oriented. When multiple 3-component recordings are available (either in a network or an array), the

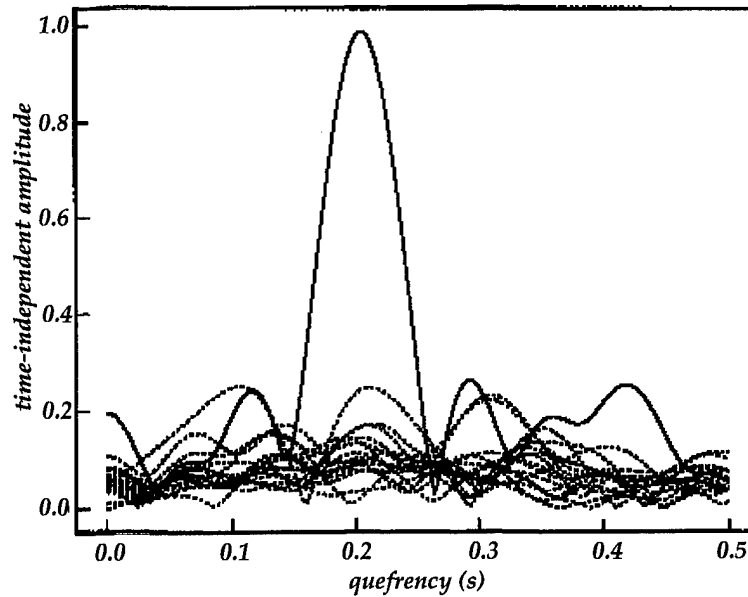


**Figure A1.** Slices through the time-independent portions of two-dimensional "coda" cepstra computed from a quarry blast and all the earthquakes considered in *Hedlin et al (1990)*. The quarry blast sonogram contains a significant amount of time independent energy at a quefrequency of 0.2 s.

individual estimates (*e.g.* of the cross correlation between vertical and east-west) are averaged together to obtain a more stable estimate. Thus, regardless of the nature of the seismic 3-component deployment, cross-correlation yields three parameters for discrimination.

*Time Independence and Periodicity in Frequency.* These qualities are estimated together by using the coda cepstrum. The cepstrum is calculated by taking the Fourier transform of the log (base 10) of a single, detrended, spectral estimate (*Tribolet, 1979; Baumgardt & Ziegler, 1988*). The coda cepstrum (as defined by *Hedlin et al., 1995*) is calculated by taking the two-dimensional Fourier transform of the binary sonogram (which is detrended by the conversion into binary form). The two-dimensional coda cepstrum is sensitive to spectral periodicities which are constant, or cyclic, with time in the onset phases and coda. To estimate the degree to which time-independent scallops are present we take the maximum of the coda cepstrum at a time-frequency of zero (Figure A.1). This value is normalized relative to the maximum of the coda cepstrum calculated from a synthetic binary sonogram (which has the same periodicity in frequency and is independent of time, with the exception that the randomization mask applied to the real sonogram is also applied to the synthetic). The quefrequency of the maximum can be used to estimate a dominant delay-fire delay or source duration. When the event has been recorded by numerous sensors, the cepstral values are averaged together. Thus, when applied to a single component deployment, the coda cepstrum will yield a single parameter. A 3-component deployment, averaged in the same fashion, will yield three.

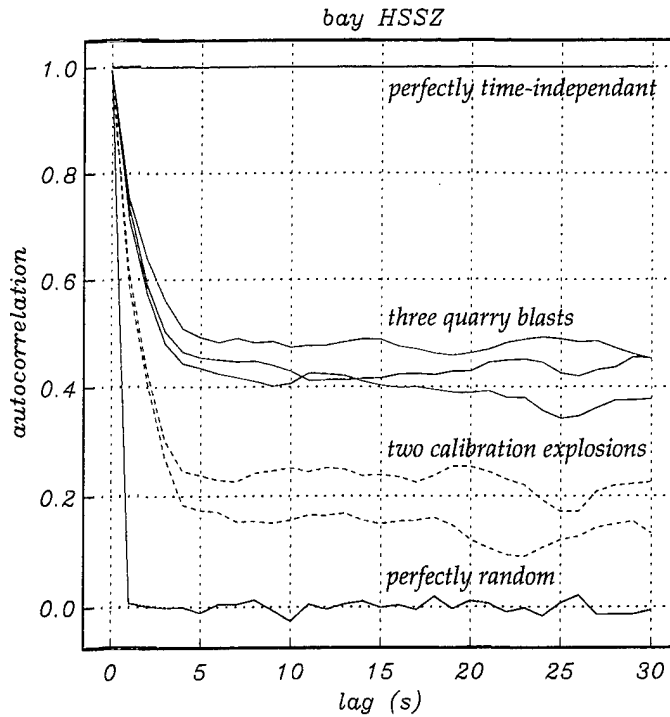


**Figure A2.** The autocorrelations calculated for three quarry blasts and two calibration explosions recorded during the 1987 NRDC experiment. All recordings were made at high gain by the surface sensor at Bayanaul. Also plotted are the autocorrelations for a perfectly random pattern and one for a perfectly time-independent pattern.

For an additional measure of time-independence we apply an autocorrelation operator to the binary matrix,  $B(f, t)$ , where the autocorrelation at a lag of  $k$  windows,  $A(k)$ , is given by:

$$A(k) = \frac{\sum_{i=1}^{n_{freq}} \sum_{j=1}^{n_{time}-k} B(i, j) B(i, j+k) R(i, j) R(i, j+k)}{\sum_{i=1}^{n_{freq}} \sum_{j=1}^{n_{time}-k} R(i, j) R(i, j+k)}$$

Considering events recorded by the NRDC network (dataset 1; *Hedlin et al., 1989*) we have found that the autocorrelation does not depend on the lag (provided that the lags are large enough to ensure no window overlap; Figure A.2). In practice, when using 2.5 second windows with 20% overlap, we use minimum lag of 6 windows and a maximum equal to the duration of the sonogram). All pairs which include a point that has been randomized, due to noise, are excluded. For a robust estimate of  $A$  we average over all appropriate lags. As above, autocorrelation yields a single averaged parameter (or three if the deployment has 3-component stations).

With the measures described above, the ATFD yields nine parameters when applied to a 3-component deployment or just two (one each from the coda-cepstrum and autocorrelation) when single component data are available. These parameters are merged using multivariate statistics. The ATFD is trained in a new region by processing a number of known quarry blasts and earthquakes and/or calibration explosions. In effect, the ATFD is taught to recognize the binary patterns produced by the two types of events (delay-fired/non-delay-fired).

THOMAS AHRENS  
SEISMOLOGICAL LABORATORY 252-21  
CALIFORNIA INST. OF TECHNOLOGY  
PASADENA, CA 91125

AIR FORCE RESEARCH LABORATORY  
ATTN: VSOE  
29 RANDOLPH ROAD  
HANSCOM AFB, MA 01731-3010  
(2 COPIES)

AIR FORCE RESEARCH LABORATORY  
ATTN: RESEARCH LIBRARY/TL  
5 WRIGHT STREET  
HANSCOM AFB, MA 01731-3004

AIR FORCE RESEARCH LABORATORY  
ATTN: AFRL/SUL  
3550 ABERDEEN AVE SE  
KIRTLAND AFB, NM 87117-5776  
(2 COPIES)

RALPH ALEWINE  
NTPO  
1901 N. MOORE STREET, SUITE 609  
ARLINGTON, VA 22209

MUAWIA BARAZANGI  
INSTOC  
3126 SNEE HALL  
CORNELL UNIVERSITY  
ITHACA, NY 14853

T.G. BARKER  
MAXWELL TECHNOLOGIES  
8888 BALBOA AVE.  
SAN DIEGO, CA 92123-1506

DOUGLAS BAUMGARDT  
ENSCO INC.  
5400 PORT ROYAL ROAD  
SPRINGFIELD, VA 22151

THERON J. BENNETT  
MAXWELL TECHNOLOGIES  
11800 SUNRISE VALLEY DRIVE, STE 1212  
RESTON, VA 22091

WILLIAM BENSON  
NAS/COS  
ROOM HA372  
2001 WISCONSIN AVE. NW  
WASHINGTON DC 20007

JONATHAN BERGER  
UNIVERSITY OF CA, SAN DIEGO  
SCRIPPS INST. OF OCEANOGRAPHY  
IGPP, 0225  
9500 GILMAN DRIVE  
LA JOLLA, CA 92093-0225

ROBERT BLANDFORD  
AFTAC  
1300 N. 17TH STREET  
SUITE 1450  
ARLINGTON, VA 22209-2308

LESLIE A. CASEY  
DEPT. OF ENERGY/NN-20  
1000 INDEPENDENCE AVE. SW  
WASHINGTON DC 20585-0420

CENTER FOR MONITORING RESEARCH  
ATTN: LIBRARIAN  
1300 N. 17th STREET, SUITE 1450  
ARLINGTON, VA 22209

ANTON DAINITY  
HQ DSWA/PMA  
6801 TELEGRAPH ROAD  
ALEXANDRIA, VA 22310-3398

CATHERINE DE GROOT-HEDLIN  
UNIV. OF CALIFORNIA, SAN DIEGO  
INST. OF GEOP. & PLANETARY PHYSICS  
8604 LA JOLLA SHORES DRIVE  
SAN DIEGO, CA 92093

DTIC  
8725 JOHN J. KINGMAN ROAD  
FT BELVOIR, VA 22060-6218 (2 COPIES)

DIANE DOSER  
DEPT OF GEOLOGICAL SCIENCES  
THE UNIVERSITY OF TEXAS AT EL PASO  
EL PASO, TX 79968

MARK D. FISK  
MISSION RESEARCH CORPORATION  
735 STATE STREET  
P.O. DRAWER 719  
SANTA BARBARA, CA 93102-0719

LORI GRANT  
MULTIMAX, INC.  
311C FOREST AVE. SUITE 3  
PACIFIC GROVE, CA 93950

HENRY GRAY  
SMU STATISTICS DEPARTMENT  
P.O. BOX 750302  
DALLAS, TX 75275-0302

I. N. GUPTA  
MULTIMAX, INC.  
1441 MCCORMICK DRIVE  
LARGO, MD 20774

DAVID HARKRIDER  
BOSTON COLLEGE  
INSTITUTE FOR SPACE RESEARCH  
140 COMMONWEALTH AVENUE  
CHESTNUT HILL, MA 02167

THOMAS HEARN  
NEW MEXICO STATE UNIVERSITY  
DEPARTMENT OF PHYSICS  
LAS CRUCES, NM 88003

MICHAEL HEDLIN  
UNIV. OF CALIFORNIA, SAN DIEGO  
SCRIPPS INST. OF OCEANOGRAPHY  
IGPP, 0225  
9500 GILMAN DRIVE  
LA JOLLA, CA 92093-0225

DONALD HELMBERGER  
CALIFORNIA INST. OF TECHNOLOGY  
DIV. OF GEOL. & PLANETARY SCIENCES  
SEISMOLOGICAL LABORATORY  
PASADENA, CA 91125

EUGENE HERRIN  
SOUTHERN METHODIST UNIVERSITY  
DEPARTMENT OF GEOLOGICAL  
SCIENCES  
DALLAS, TX 75275-0395

ROBERT HERRMANN  
ST. LOUIS UNIVERSITY  
DEPT OF EARTH & ATMOS. SCIENCES  
3507 LACLEDE AVENUE  
ST. LOUIS, MO 63103

VINDELL HSU  
HQ/AFTAC/TTR  
1030 S. HIGHWAY A1A  
PATRICK AFB, FL 32925-3002

RONG-SONG JIH  
HQ DSWA/PMA  
6801 TELEGRAPH ROAD  
ALEXANDRIA, VA 22310-3398

THOMAS JORDAN  
MASS. INST. OF TECHNOLOGY  
BLDG 54-918  
77 MASSACHUSETTS AVENUE  
CAMBRIDGE, MA 02139

LAWRENCE LIVERMORE NAT'L LAB  
ATTN: TECHNICAL STAFF (PLS ROUTE)  
PO BOX 808, MS L-175  
LIVERMORE, CA 94551

LAWRENCE LIVERMORE NAT'L LAB  
ATTN: TECHNICAL STAFF (PLS ROUTE)  
PO BOX 808, MS L-208  
LIVERMORE, CA 94551

LAWRENCE LIVERMORE NAT'L LAB  
ATTN: TECHNICAL STAFF (PLS ROUTE)  
PO BOX 808, MS L-202  
LIVERMORE, CA 94551

LAWRENCE LIVERMORE NAT'L LAB  
ATTN: TECHNICAL STAFF (PLS ROUTE)  
PO BOX 808, MS L-195  
LIVERMORE, CA 94551

LAWRENCE LIVERMORE NAT'L LAB  
ATTN: TECHNICAL STAFF (PLS ROUTE)  
PO BOX 808, MS L-205  
LIVERMORE, CA 94551

LAWRENCE LIVERMORE NAT'L LAB  
ATTN: TECHNICAL STAFF (PLS ROUTE)  
PO BOX 808, MS L-200  
LIVERMORE, CA 94551

LAWRENCE LIVERMORE NAT'L LAB  
ATTN: TECHNICAL STAFF (PLS ROUTE)  
PO BOX 808, MS L-221  
LIVERMORE, CA 94551

THORNE LAY  
UNIV. OF CALIFORNIA, SANTA CRUZ  
EARTH SCIENCES DEPARTMENT  
EARTH & MARINE SCIENCE BUILDING  
SANTA CRUZ, CA 95064

ANATOLI L. LEVSHIN  
DEPARTMENT OF PHYSICS  
UNIVERSITY OF COLORADO  
CAMPUS BOX 390  
BOULDER, CO 80309-0309

JAMES LEWKOWICZ  
WESTON GEOPHYSICAL CORP.  
325 WEST MAIN STREET  
NORTHBORO, MA 01532

LOS ALAMOS NATIONAL LABORATORY  
ATTN: TECHNICAL STAFF (PLS ROUTE)  
PO BOX 1663, MS F659  
LOS ALAMOS, NM 87545

LOS ALAMOS NATIONAL LABORATORY  
ATTN: TECHNICAL STAFF (PLS ROUTE)  
PO BOX 1663, MS F665  
LOS ALAMOS, NM 87545

LOS ALAMOS NATIONAL LABORATORY  
ATTN: TECHNICAL STAFF (PLS ROUTE)  
PO BOX 1663, MS C335  
LOS ALAMOS, NM 87545

GARY MCCARTOR  
SOUTHERN METHODIST UNIVERSITY  
DEPARTMENT OF PHYSICS  
DALLAS, TX 75275-0395

KEITH MCLAUGHLIN  
CENTER FOR MONITORING RESEARCH  
SAIC  
1300 N. 17TH STREET, SUITE 1450  
ARLINGTON, VA 22209

BRIAN MITCHELL  
DEPT OF EARTH & ATMOS. SCIENCES  
ST. LOUIS UNIVERSITY  
3507 LACLEDE AVENUE  
ST. LOUIS, MO 63103

RICHARD MORROW  
USACDA/IVI  
320 21ST STREET, N.W.  
WASHINGTON DC 20451

JOHN MURPHY  
MAXWELL TECHNOLOGIES  
11800 SUNRISE VALLEY DRIVE, STE 1212  
RESTON, VA 22091

JAMES NI  
NEW MEXICO STATE UNIVERSITY  
DEPARTMENT OF PHYSICS  
LAS CRUCES, NM 88003

ROBERT NORTH  
CENTER FOR MONITORING RESEARCH  
1300 N. 17th STREET, SUITE 1450  
ARLINGTON, VA 22209

OFFICE OF THE SECRETARY OF DEFENSE  
DDR&E  
WASHINGTON DC 20330

JOHN ORCUTT  
INST. OF GEOPH. & PLANETARY PHYSICS  
UNIV. OF CALIFORNIA, SAN DIEGO  
LA JOLLA, CA 92093

PACIFIC NORTHWEST NAT'L LAB  
ATTN: TECHNICAL STAFF (PLS ROUTE)  
PO BOX 999, MS K6-48  
RICHLAND, WA 99352

PACIFIC NORTHWEST NAT'L LAB  
ATTN: TECHNICAL STAFF (PLS ROUTE)  
PO BOX 999, MS K6-40  
RICHLAND, WA 99352

PACIFIC NORTHWEST NAT'L LAB  
ATTN: TECHNICAL STAFF (PLS ROUTE)  
PO BOX 999, MS K6-84  
RICHLAND, WA 99352

PACIFIC NORTHWEST NAT'L LAB  
ATTN: TECHNICAL STAFF (PLS ROUTE)  
PO BOX 999, MS K5-12  
RICHLAND, WA 99352

FRANK PILOTTE  
HQ AFTAC/TT  
1030 S. HIGHWAY A1A  
PATRICK AFB, FL 32925-3002

KEITH PRIESTLEY  
DEPARTMENT OF EARTH SCIENCES  
UNIVERSITY OF CAMBRIDGE  
MADINGLEY RISE, MADINGLEY ROAD  
CAMBRIDGE, CB3 0EZ UK

JAY PULLI  
BBN SYSTEMS AND TECHNOLOGIES, INC.  
1300 NORTH 17TH STREET  
ROSSLYN, VA 22209



DELAINE REITER  
AFRL/VSOE (SENCOM)  
29 RANDOLPH ROAD  
HANSCOM AFB, MA 01731-3010

PAUL RICHARDS  
COLUMBIA UNIVERSITY  
LAMONT-DOHERTY EARTH OBSERV.  
PALISADES, NY 10964

MICHAEL RITZWOLLER  
DEPARTMENT OF PHYSICS  
UNIVERSITY OF COLORADO  
CAMPUS BOX 390  
BOULDER, CO 80309-0309

DAVID RUSSELL  
HQ AFTAC/TTR  
1030 SOUTH HIGHWAY A1A  
PATRICK AFB, FL 32925-3002

CHANDAN SAIKIA  
WOODWARD-CLYDE FED. SERVICES  
566 EL DORADO ST., SUITE 100  
PASADENA, CA 91101-2560

SANDIA NATIONAL LABORATORY  
ATTN: TECHNICAL STAFF (PLS ROUTE)  
DEPT. 5704  
MS 0979, PO BOX 5800  
ALBUQUERQUE, NM 87185-0979

SANDIA NATIONAL LABORATORY  
ATTN: TECHNICAL STAFF (PLS ROUTE)  
DEPT. 9311  
MS 1159, PO BOX 5800  
ALBUQUERQUE, NM 87185-1159

SANDIA NATIONAL LABORATORY  
ATTN: TECHNICAL STAFF (PLS ROUTE)  
DEPT. 5704  
MS 0655, PO BOX 5800  
ALBUQUERQUE, NM 87185-0655

SANDIA NATIONAL LABORATORY  
ATTN: TECHNICAL STAFF (PLS ROUTE)  
DEPT. 5736  
MS 0655, PO BOX 5800  
ALBUQUERQUE, NM 87185-0655

THOMAS SERENO, JR.  
SAIC  
10260 CAMPUS POINT DRIVE  
SAN DIEGO, CA 92121

AVI SHAPIRA  
SEISMOLOGY DIVISION  
IPRG  
P.O.B. 2286  
NOLON 58122 ISRAEL

ROBERT SHUMWAY  
410 MRAC HALL  
DIVISION OF STATISTICS  
UNIVERSITY OF CALIFORNIA  
DAVIS, CA 95616-8671

MATTHEW SIBOL  
ENSCO, INC.  
445 PINEDA CT.  
MELBOURNE, FL 32940

DAVID SIMPSON  
IRIS  
1200 NEW YORK AVE., NW  
SUITE 800  
WASHINGTON DC 20005

JEFFRY STEVENS  
MAXWELL TECHNOLOGIES  
8888 BALBOA AVE.  
SAN DIEGO, CA 92123-1506

BRIAN SULLIVAN  
BOSTON COLLEGE  
INSTITUTE FOR SPACE RESEARCH  
140 COMMONWEALTH AVENUE  
CHESTNUT HILL, MA 02167

TACTEC  
BATTELLE MEMORIAL INSTITUTE  
505 KING AVENUE  
COLUMBUS, OH 43201 (FINAL REPORT)

NAFI TOKSOZ  
EARTH RESOURCES LABORATORY, M.I.T.  
42 CARLTON STREET, E34-440  
CAMBRIDGE, MA 02142

LAWRENCE TURNBULL  
ACIS  
DCI/ACIS  
WASHINGTON DC 20505

GREG VAN DER VINK  
IRIS  
1200 NEW YORK AVE., NW  
SUITE 800  
WASHINGTON DC 20005

FRANK VERNON  
UNIV. OF CALIFORNIA, SAN DIEGO  
SCRIPPS INST. OF OCEANOGRAPHY  
IGPP, 0225  
9500 GILMAN DRIVE  
LA JOLLA, CA 92093-0225

TERRY WALLACE  
UNIVERSITY OF ARIZONA  
DEPARTMENT OF GEOSCIENCES  
BUILDING #77  
TUCSON, AZ 85721

JILL WARREN  
LOS ALAMOS NATIONAL LABORATORY  
GROUP NIS-8  
P.O. BOX 1663  
LOS ALAMOS, NM 87545 (5 COPIES)

DANIEL WEILL  
NSF  
EAR-785  
4201 WILSON BLVD., ROOM 785  
ARLINGTON, VA 22230

RU SHAN WU  
UNIV. OF CALIFORNIA SANTA CRUZ  
EARTH SCIENCES DEPT.  
1156 HIGH STREET  
SANTA CRUZ, CA 95064

JIAKANG XIE  
COLUMBIA UNIVERSITY  
LAMONT DOHERTY EARTH OBSERV.  
ROUTE 9W  
PALISADES, NY 10964

JAMES E. ZOLLWEG  
BOISE STATE UNIVERSITY  
GEOSCIENCES DEPT.  
1910 UNIVERSITY DRIVE  
BOISE, ID 83725